How Subtle Can It Get? A Trimodal Study of Ring-sized Interfaces for One-Handed Drone Control

YUI-PAN YAU*, Department of Computer Science and Engineering, The Hong Kong University of Science and Technology, Hong Kong
LIK HANG LEE†, Center for Ubiquitous Computing, The University of Oulu, Finland
ZHENG LI, Department of Computer Science and Engineering, The Hong Kong University of Science and Technology, Hong Kong and Fudan University, Shanghai, China
TRISTAN BRAUD, Department of Computer Science and Engineering, The Hong Kong University of Science and Technology, Hong Kong
YI-HSUAN HO, Department of Computer Science and Engineering, The Hong Kong University of Science and Technology, Hong Kong
PAN HUI, Department of Computer Science and Engineering, The Hong Kong University of Science and Technology, Hong Kong and Department of Computer Science, The University of Helsinki, Finland

Flying drones have become common objects in our daily lives, serving a multitude of purposes. Many of these purposes involve outdoor scenarios where the user combines drone control with another activity. Traditional interaction methods rely on physical or virtual joysticks that occupy both hands, thus restricting drone usability. In this paper, we investigate one-handed human-to-drone-interaction by leveraging three modalities: force, touch, and IMU. After prototyping three different combinations of these modalities on a smartphone, we evaluate them against the current commercial standard through two user experiments. These experiments help us to find the combination of modalities that strikes a compromise between user performance, perceived task load, wrist rotation, and interaction area size. Accordingly, we select a method that achieves faster task completion times than the two-handed commercial baseline by 16.54% with the merits of subtle user behaviours inside a small-size ring-form device and implements this method within the ring-form device. The last experiment involving 12 participants shows that thanks to its small size and weight, the ring device displays better performance than the same method implemented on a mobile phone. Furthermore, users unanimously found the device useful for controlling a drone in mobile scenarios (AVG = 3.92/5), easy to use (AVG = 3.58/5) and easy to learn (AVG = 3.58/5). Our findings give significant design clues in search of subtle and effective interaction through finger augmentation devices with drone control. The users with our prototypical system and a multi-modal on-finger device can control a drone with subtle wrist rotation

*Yui-Pan YAU and Lik Hang LEE contributed equally to this work.
†This is the corresponding author: lik.lee@oulu.fi.

Authors' addresses: Yui-Pan Yau Department of Computer Science and Engineering, The Hong Kong University of Science and Technology, Hong Kong; Lik Hang Lee Center for Ubiquitous Computing, The University of Oulu, Finland; Zheng Li Department of Computer Science and Engineering, The Hong Kong University of Science and Technology, Hong Kong Fudan University, Shanghai, China; Tristan Braud Department of Computer Science and Engineering, The Hong Kong University of Science and Technology, Hong Kong; Yi-Hsuan Ho Department of Computer Science and Engineering, The Hong Kong University of Science and Technology, Hong Kong; Pan Hui Department of Computer Science and Engineering, The Hong Kong University of Science and Technology, Hong Kong Department of Computer Science, The University of Helsinki, Finland.

2474-9567/2020/6-ART63 $15.00
https://doi.org/10.1145/3397319

(pitch gestures: 43.24° amplitude and roll gestures: 46.35° amplitude) and unnoticeable thumb presses within a miniature-sized area of (1.08 * 0.61 cm^2).

CCS Concepts: • **Computer systems organization → Human-Drone Interaction**; *Interface Design*; • **Multimodal Inputs**; • **Thumb-to-finger Interaction**;

Additional Key Words and Phrases: Human-drone interaction; On-finger interaction; multi-modal inputs.

ACM Reference Format:
Yui-Pan Yau, Lik Hang Lee, Zheng Li, Tristan Braud, Yi-Hsuan Ho, and Pan Hui. 2020. How Subtle Can It Get? A Trimodal Study of Ring-sized Interfaces for One-Handed Drone Control. *Proc. ACM Interact. Mob. Wearable Ubiquitous Technol.* 4, 2, Article 63 (June 2020), 29 pages. https://doi.org/10.1145/3397319

1 INTRODUCTION

Flying drones are currently proliferating in the commercial market. Drones have diverse purposes, including art display, drone racing, goods delivery, building surveying, wildfire detection, and agriculture. Fine-grained position control is important for the majority of Human-Drone Interaction or other devices for human-centered computing. The drone's position can be adjusted through four approaches: direct position control, absolute position control, relative position control, and task-oriented control [26]. Most consumer-market drones rely on direct position control. The user manipulates the position of the drone through an interface such as a tangible joystick controller. However, tangible joystick controllers are bulky and occupy both of the user's hands. In other words, users cannot hold other things or handle other tasks simultaneously. To address this issue, the research community has studied alternative interaction approaches relying on new modalities and controller form factors. A recent survey on human-drone interaction [58] reveals multiple alternative interaction modalities, among which are natural user interfaces such as voice commands [48], body gestures [13], and gestures within a finger space [22]. Although natural interfaces are intuitive [22], they tend to result in higher dwell times than tangible interfaces [50]. Also, natural user interfaces often require users to hold static gestures and thus deteriorate the user mobility. One promising solution lies in designing small-sized tangible interfaces within the finger space [70]. Indeed, such interfaces conserve the strengths of natural gestures while enhancing the responsiveness of drone controls inherited from tangible interfaces.

In this paper, we consider the premises of small-size tangible interfaces and investigate the design space for the direct position control of a flying drone with on-finger devices. A key design challenge lies in the fact that flying drones move with six-degrees of freedom (6DOF): longitudinal (forward and backward), vertical (upward and downward), lateral (right and left) directions, and rotational (right and left) movements. Two-handed tangible joysticks can easily map the 8 directional and rotational movements above. In contrast, on-finger devices offer limited space to accommodate such rich input options with thumb-sized buttons. To achieve this goal, we consider three modalities: touch, force, and inertial measurement unit (IMU). We design four candidate interaction models, and evaluate them in terms of user performance, perceived task load, and the size of the interaction areas through both unit testing and complex tasks. We evaluate our solutions on a smartphone with two separate experiments involving a total of 32 participants. In the first experiment, the 12 participants with the selected method achieve a significantly faster (16.54%) task completion time than with the two-handed approaches. In the second experiment with 20 participants, the selected method successfully reduces the size of the interaction area by 62.7% (1.08 * 0.61 cm^2), compared to the two-handed approaches. We then select the best candidate solution to design an on-finger hardware interface for thumb-to-index finger interaction. This interface consists of a single thumb-sized button associated with an IMU to address the 6 degrees of freedom for drone control. This paper specifically focuses on thumb-to-index finger interactions on a miniature-size device that enables the users to control the drone with enhanced mobility. Unlike the sizable amount of on-finger devices in the literature, this study focuses on

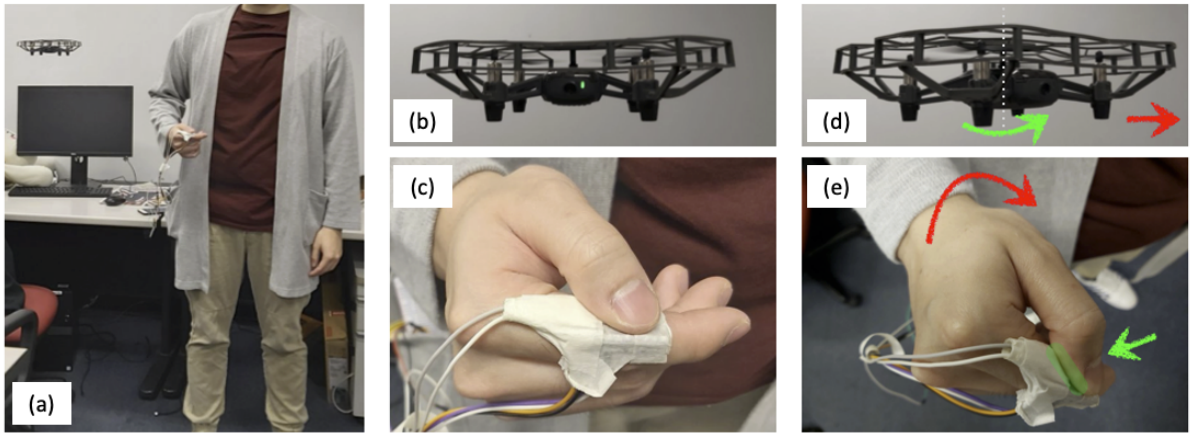

Fig. 1. An overview of the prototypical on-finger interface with a flying drone: (a) user posture with the proposed thumb-to-index finger interface; (b) a hovering drone and (c) a close-up shot of the hardware interface; (d) a left-rotating drone driven by (e) a subtle roll gesture supported by the proposed force-assisted (green arrow) and IMU-induced (red arrow) interaction method that governs the magnitude (green arrow, upper) and direction (red arrow, upper) of drone movements, respectively.

on-finger devices for human-drone interaction for the first time, leveraging the strengths of both natural user interaction and tangible interfaces.

Figure 1 gives an overview of our prototype system for the direct position control of a flying drone. The hardware interface consists of a capacitive plate with force-sensitive and touch-sensitive capabilities. The user can perform off-hand and thumb-to-index finger interactions with subtle and unnoticeable finger movements. The novelty of this on-finger device resides in the usage of force-assisted interaction, combined with subtle wrist and thumb movements. The on-finger device is designed specifically for human-to-drone-interaction, where one-thumb interaction on the finger space enables the user to reserve at least one free hand for holding objects (e.g. documents and working tools) in an outdoor scenario.

Our contribution is threefold.

- We explore and design a trimodal input method leveraging force-assisted, touch-enabled, and IMU-induced interactions on a finger-mounted interface for drone position control.
- According to the design clues collected in two user evaluations, we implement the selected method on a ring-shaped prototype system for hands-off and single-handed interaction in outdoor and mobile scenarios.
- In the final experiment, users achieve 27.99% faster performance with the lightweight prototype than with the smartphone implementation, with gentle wrist rotation for pitch gestures: (43.24° amplitude) and roll gestures: (46.35° amplitude).

The rest of this paper is organized as follows. In Section 2, we give a detailed review of the most relevant works on drone control, thumb interaction, interactions with miniature devices, as well as force-assisted interactions. In Section 3, we design and evaluate four candidate interaction models before system and hardware implementations. On the basis of the first (Section 4) and second evaluations (Section 5), we build a ring-shaped hardware prototype system in Section 6. Finally, we evaluate the system and hardware performance and discuss our findings and the design implication of this study.

2 RELATED WORK

In this section, we first discuss the existing works for controlling flying drones. We then focus on the latest works on one-thumb, one-handed and force-assisted interactions.

2.1 Drone Control

One of the most significant focus areas for human-drone interaction [74] is the use of alternative modalities for the flying drone control, for instance, hand movements [23, 29, 46, 63], body movements [40, 42, 60, 68], gaze [31], mind [45, 62], voice command [48], tangible interface [5, 18, 44, 67], and haptic feedback [2, 3].

Morishita et al. [60] collect postural data from a gyroscope and an accelerometer attached to the user's shoulder. The drone will move in the direction of the body's lean angle. Similarly, Flight Chair [40] consists of a gyroscope attached to a chair. The gyroscope detects the user's body angles while sitting on a chair to control the drone. Apart from sedentary postures like standing and sitting, Aeroquake [42] captures the dancer's body gestures such as Quaking (foot) and Waving (hand) to control a swarm of drones. Seuter et al. [68] bring control gestures in outdoor running scenarios. Considering hand movement is a natural user interface, sensing arm movements vary from pointing gestures [29], single arm movements [23] to two-handed gestures [63]. The sensors are commonly attached to wearables such as gloves [67].

Prolonged actions of body gestures can lead to fatigue and Gorilla arm [52]. More subtle interactions, such as gaze-driven and electrophysiological interfaces, pose limitations on accuracy as well as increased physical and mental demands. Voice command has drawbacks such as a diminished sense of agency [54] and limited usability in shared environments [34]. Tangible interfaces enable subtle interaction with none of the aforementioned issues. Many tangible interfaces combine with a gyroscope and an accelerometer to fly a drone in a 3D space. In DroneCTRL [44], a laser pointer embedded on a pen-like controller allows non-expert users to improve drone navigation by enabling pointing gestures. By leveraging the touchscreen interfaces and gyroscopes on smartphones [18], the user can direct the drone to take pictures. In CAGE [5], the pen-like controller is equipped with a four stepper motor to give user feedback when the drone is near hazardous objects. However, none of the tangible devices above explores the use of force as a modality to control drones.

Table 1 summarizes the most recent works for human-drone interaction, in which the existing works only employ some modalities for their study objectives but not considered the effects of modalities on the ring-sized interfaces for drone controls. Among these works, the research community paid attention to factors such as drone's movements [11, 15, 57], appearance [79], comfortable distance [4], content projections [14, 21], videography [19], and employing flying drones as companion devices[41] (e.g. pets [43]), in addition to other issues, such as privacy [81], human responses in social environments [8] and drone identification [66]. The formative studies and user surveys for eliciting natural user gestures covers multiple modalities for human-drone interaction, including voice commands and hand gestures in both the American [13] and Chinese [24] populations, as well as direct touches on the propeller guards of the drones [4]. Our paper is the first to consider the impact of force-based interaction in controlling the dynamics of a drone system with six-degree of freedom (6DOF) in the longitudinal (forward and backward), vertical (upward and downward), lateral (right and left), as well as rotational (right and left) directions. On the other hand, the existing commercial standards for two-handed (e.g. DJI) and one-handed (e.g. FT Aviator) drone control occupy the whole hand(s) of the user and are thus of limited interest in multi-tasking scenarios in outdoor. One recent example is the massive use of drones in China during the coronavirus crisis[1], which shows drone operations required two people at work, one controlling the navigation while the other performs other operations[2]. The relevant works on two-handed controllers investigate the difficulties of applying a flying drone as the pointing device in a physical environment [80] and the manipulation on the

[1] https://www.bloomberg.com/news/articles/2020-02-04/drones-take-to-china-s-skies-to-fight-coronavirus-outbreak
[2] https://youtu.be/SdZ53QFTqmo

Table 1. A summary of the most recent works of human-drone interaction, showing the study objectives and interaction devices / modality.

Ref.	Study Objectives	Interaction Devices / Modality
[43]	Investigate the questions of what characteristics drones as artificial companions should have?	*Nil,* survey
[41]	Employ a drone as a companion device for a pedestrian for the user safety, emotional responsiveness and warmth.	Bluetooth on Smartwatches
[79]	Study how the appearance and form factors of the drones impact the user perception.	*Nil*, Formative Study of 63 drones
[15]	Personalise the drone flying path and altitude depending on the user's personality traits and emotional attributes, with the ultimately goal of emulating drones as pets.	Formative Study, Pre-flight Encoding and Questionnaire
[57]	Propose an acoustic-based tracking system that enables a drone to follow a user and perform automatic video taping.	Audio (Mic)
[81]	Study how the drone users and bystanders perceive privacy concerns and eight privacy protection mechanisms.	*Nil,* two-round surveys
[24]	Investigate how the cultural differences affect user-defined interactions, using multi-modal inputs such as voice commands and hand gestures, through a Wizard of Oz study.	Audio and camera (indicative)
[13]	Elicit user hand gestures for interacting with a drone, through a Wizard of Oz study.	camera (indicative)
[4]	Study the feasibility and user perceptions for the potential use of propeller guards on a drone as a novel touch interfaces.	Gesture, Audio, Direct Touch on the propeller guards
[73]	Design a third-person piloting interfaces in which a small-size toy drone as a tangible yet manipulatable interfaces is attached to a two-handed tangible controller, in order to facilitate the flight of another large and professional drone and enhance the user's spatial comprehension.	A Two-handed tangible controllers for directional controls, plus a toy drone for spatial relationship
[80]	Employ a drone as a pointing device in the 3D space for the Fitts' Law studying the effect of target distance and target width to the movement time and error rate of the drone pointing action.	A Two-handed tangible controller
[66]	Propose a robust physical drone identification system through motion matching and actuation feedback.	*Nil*, Drone-to-drone interaction using ID systems

tangible interfaces of a toy drone for better spatial awareness [73]. Alternative controllers designated for Virtual Reality enables users to script the drone routine before the flights [32]. In contrast, our proposed work aims to construct a miniature interface driven by one-handed and subtle interaction, by investigating the following modalities: IMU-driven, force-assisted and touch-based interfaces. The ring-form interface allows users to quickly switch to physical tasks requiring two hands.

2.2 Thumb Interactions with Mobile Computers

Among the research works on thumb interaction in the domain of mobile Human-Computer Interaction, the thumb gestures and thumb reaches on smartphones have been widely studied [53]. In FatThumb [10], a touchscreen device detects the thumb contact areas to interpret the user gestures on a map application either as a simple tap or a pinch gesture for zooming. Gestures considering limited thumb reach with the firm grip on smartphones address the ergonomics of the carpometacarpal (CMC) joint, the metacarpophalangeal (MCP) and the interphalangeal

(IP) joint [49]. For instance, MagStick [65] applies drag gestures to project a linear trajectory to reach a target on the farthest area of a smartphone interface.

In recent years, the research community on on-body interaction has been studying the design space of thumb-to-finger interactions, which is regarded as subtle, swift, and unnoticeable interactions [50]. In [70], thumb reaches to different fingers within the same hand are classified into a set of micro-gestures that maps with instructions on computing devices. Chan et al. [16] analyze the thumb reaches inside the finger space, considering the ease of thumb reaches to distal segments, middle segments and proximal segments of the index finger, middle finger, ring finger as well as small finger. Karlson et al. [39] reveal similar results with a further study on the thumb to the dorsal and radial sides of the finger space. Thumb-to-finger and thumb-to-palm interactions have also been considered for text entry on mobile devices [51, 77, 78]. With very few works focusing on thumb-to-finger interaction, this paper serves as the first works to leverage the benefits of thumb interaction with flying drones.

2.3 One-handed Interaction on Miniature Devices

A large number of Finger-Augmenting Devices (FAD) have been proposed [69], which are commonly attached either to the finger (partially or fully covered depending on the size of the devices) or the thumb with an addendum sensor located on the nail. FingerPad [17] enables gesture recognition through magnetic tracking between the Hall sensor grid and magnets on the fingernails of the thumb and index finger. Among the FADs, ring devices are the most acceptable and practical ubiquitous wearable device, and allow hand-free operations in outdoors scenarios [7]. Commercial products are widely used in health tracking[3] and voice assistant[4]. Magic Ring [38] analyzes the user movements with IMU sensor data to recognize real-life activities such as tooth brushing and cooking noodles. Frictio [30] generates passive kinesthetic force feedback when users perform IMU-supported rotational gestures on desktop computers.

Among thumb-to-index finger interaction, touch is the primary input modality on ring devices. The printed electrodes and capacitive sensors inside TouchRing [76] enable the detection of touch events and swipe gestures. Ringteraction [27] achieves more complicated event detection including taps, swipes, rotations, scroll and select, pan and zoom, and so on. Thumb-In-Motion [9] inherits from the above works and reduces the form-size for outdoor scenarios (e.g. walking and running). These projects demonstrate touch-based gesture recognition with tapping and swipe motions with static 2D GUIs. In contrast, our prototype applies force-assisted interaction with dynamic tangible objects like flying drones.

Among the CMC, IP and MCP joints, Karlson et al. [39] show evidence that rubbing the thumb inside the hand space (palm or some fingers) diagonally and horizontally is more demanding and leads to a longer completion time, which implies that the bottleneck with the thumb's IP and MCP joints for rigorous motions deteriorates the user performance. The aforementioned TouchRing, Ringteraction and Thumb-In-Motion rely on rigorous motions for tap and swipe gestures involving IP and MCP joints. In contrast, multi-modal inputs with touch-based, force-assisted interaction supported by an IMU allow for subtle movements on the interface, thus reducing the burden on such joints.

2.4 Force-Assisted Interaction

When fingers exert force on a surface, the sensory receptors of the muscles located predominantly outside the hand provide constant feedback to the user on the amount of force exerted [1]. Humans are capable of distinguishing between subtle amounts of force up to 6 levels [59] with only visual clues and potentially reach up to 10 levels [82] with adequate feedback. The human finger can generate pressure averaging 45N for men and 17N for women [71], much higher than the ceiling of 3D Touch (3.3N) on an iPhone 6 or later versions [75].

[3]BELUN: http://beluntech.com
[4]ORII: https://orii.io

Table 2. A Summary of Sensing Capacities and the Key Gestures.

Models	Touch-sensitive	Force-sensitive	IMU	No. of Buttons	Interactions/Gestures
M1	x			2	Pan.
M2	x		x	1	Pan; Roll; Pitch.
M3	x	x	x	1	Pan; 3D Touch; Roll; Pitch.
M4		x	x	1	3D Touch; Roll; Pitch

Research on force-sensitive touch interfaces uses force as a modality to distinguish multiple choices through variations of the applied pressure in a continuous spectrum. The most recent and relevant works focus on shrinking the interaction areas. ForceEdge [6] enables users to scroll within a list of items (e.g. date) through exerting force on a force-sensitive touchscreen. Instead of performing one or more swipe gestures to scroll the list of items, a finger is held on the same interaction area and force is exerted to search through the list. Similarly, Goguey et al. [28] apply force-augmented taps to select the granularity of textual contents on touchscreens. The user can hold a pan gesture to select textual contents at the desired granularity. Some works apply force to perform mode switching on the keyboard interfaces. In a keyboard proposed by Brewster et al. [12], the user can apply force to type uppercase letters without tapping the 'shift' key in advance, saving time from an additional tap on the 'shift' key. Force levels can also be applied for distinguishing multiple characters in an ambiguous keyboard, in which a key contains two [35] or three characters [51]. The ambiguous keyboard reduces the keyboard size as character keys are grouped together. As such, they are favoured by smaller devices such as smartwatches and other wearable devices. In addition, force interaction improves reachability with a firm grip. ForceRay applies a force-driven cursor allowing users to access items located outside of thumb reach, following the natural rotation around the carpometacarpal joint [20]. However, none of these studies leverage the advantages of force input to tackle drone control with one-handed gestures. To the best of our knowledge, this is the first work to explore the force modality and construct a thumb-sized interface for drone interactions.

3 DESIGN OF INTERACTION MODELS

Before we dive into the hardware design of our ring, we first study the appropriate interaction approaches with flying drones for thumb-based interaction on a thumb-sized interface. In this section, we investigate four candidate interaction models for one-handed control of a flying drone. Among the four models, the first model emulates the commercial standard of two-button (two-thumbs) controllers on a smartphone touchscreen, while the remaining three solutions are one-button (one-thumb) interfaces designed for evaluating the user performance with various combinations of the Inertial Measurement Unit (IMU), the touchscreen and the force-sensitive touch surface. Table 2 summarizes the interaction approaches, their use of sensing capacities, and the key gestures.

Model 1. This model corresponds with the commercial baseline that we compare with other proposed models in this paper. The interface of this model consists of two circular virtual joysticks of diameter 37.72 mm that will be referred to as controllers. The centre points of the left controller and right controller are located at (120 pt, 130 pt) and (616 pt, 130 pt) on a 414x736 pt^2 touchscreen. The left controller controls the altitude and rotation of the flying drone, through pan gesture in four discrete directions (up, down, right, left). Panning Up and Down increases and decreases the drone altitude, while panning right and left leads to the drone rotating rightward and leftward. The right controller governs the horizontal movement of the drone in four directions, and the pan gesture (up, down, right, left) intuitively maps to the drone movement (forward, backward, right, left). For all the above thumb-based panning, we apply a linear interpolation to map the thumb movements with the magnitude of drone movements. The swipe length of the pan gesture from the initial touchpoint inside the button to the

current touchpoint near the circular edge is computed as the Euclidean distance, i.e. the drone moves at the highest speed if the thumb is located at the edge, or vice versa.

Model 2. As a flying drone can move longitudinally (forward and backward), vertically (upward and downward), laterally (right and left), as well as rotationally (right and left), a single-button button with a solely touch-sensitive interface can hardly accommodate the eight movement options. It is important to note that dividing the button into eight directional capabilities causes unintended inputs due to the smaller division for each partition. Therefore, an additional modality is necessary to augment the touch-sensitive interface. In this model, we leverage the IMU capabilities to distinguish the drone movements with a single button of diameter 37.72 mm. In this model, the touchscreen interface enables the longitudinal and lateral movements of the drone through panning gestures towards up, down, right and left that respectively map to the forward, backward, right and left drone movements. Similar to Model 1, the magnitude of drone movements corresponds to the swipe length from the location of initial/first touch on the button to the point of current touch location towards the button edge. Regarding the IMU-induced controls, the pitch (up and down) and roll (right and left) gestures manage the vertical and rotational movements respectively. Yaw gestures are not considered due to mobility constraints: a user in a walking scenario will turn left and right frequently, and yaw gesture will lead to confusing inputs to the drone. We define the default angles of the pitch and roll gestures as 0° and 0°. The angle ranges for the pitch and roll gestures are (-10° – +20°) and (-15° – +15°). Linear interpolation is applied to map the degree of pitch and roll with the magnitude of the drone movements vertically and rotationally.

Model 3. This one-button model leverages both the touch-sensitive surface, IMU and force-sensitive surface, in order to manage the eight options of the drone movements. The force-sensitive surface is normalized to the force spectrum from 0 to 1, which serves to divide the button into two separate levels. Force exertion below 0.2 is defined as the region of normal touch, in which the users make the pan gestures for longitudinal and lateral movements of the drone. Similar to Model 2, the touchscreen interface enables the longitudinal and lateral movements of the drone through panning gestures towards up, down, right and left that respectively map to the drone movement forward, backward, right and left. Again, the magnitude of drone movements is computed by the swipe length from the location of initial/first touch on the button to the point of current touch location towards the button edge. The button has a diameter of 37.72 mm. Once the force level exceeds the threshold value of 0.2, the IMU sensor activates to detect the wrist movement for the vertical and rotational movements. For both the pitch (up and down) and roll (right and left) gestures, the IMU serves to detect the wrist direction and the amount of force exerted by the users indicates the magnitude of drone movements. The movement speed of the drone is linearly interpolated to the normalized force spectrum from 0.2 to 1. Again, the default angles of the pitch and roll gestures are defined as 0° and 0°. Also, the angle ranges for activating the pitch gestures are +20° for upward movements and -10° for downward movements, while the activation of roll gestures happens once the wrist moves beyond +15° for right-rotation and -15° for left-rotation. Yaw gestures are neglected to avoid confusing operations with the drone.

Model 4. This model uses only an IMU and force-sensitive surface and not a touch-sensitive surface. Hence, the model no longer supports pan gestures. The wrist angle detected by the IMU transforms into a normalized spectrum from -1 to 1 for both pitch and roll gestures. Four directional movements exist with the combination of two gestures in two directions; representing (-1 to 0) and (0 to 1). The default angles of the pitch and roll gestures are 0° and 0°. In order to make 8 movement options available, every normalized direction, either (-1 to 0) or (0 to 1), is further divided into two sub-regions, where the range from 0 to the threshold is regarded as the inner region, and the range between the threshold and 1 is defined as the outer region. Regarding the drone operations, the pitch gestures map to the drone movement forward (up-inner), backward (down-inner), upward (up-outer) and downward (down-outer). The angle ranges of inner regions are (+5° – -20°) and (+15° – +40°), while the angle

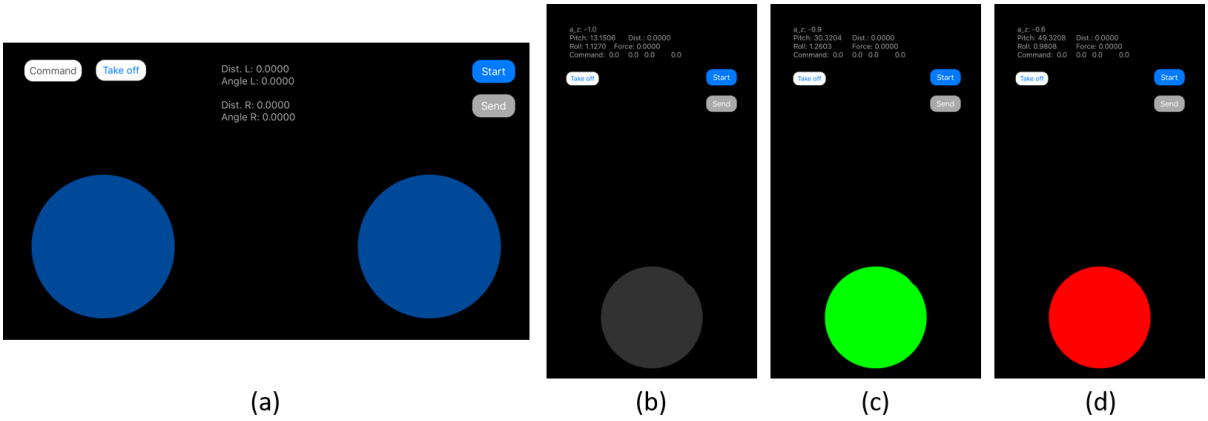

Fig. 2. Testing interfaces: (a) two-button approach for Method 1 (M1); (b) single-button approach without triggering the IMU threshold for Method 2 – 4 (M2 – M4); (c) single-button approach triggered the IMU threshold for M2 – M4; (d) single-button approach triggered the 2nd-level IMU threshold (outer region) for M4;

ranges of outer regions are (+40° – +90°) and (-20° – -90°). On the other hand, the roll gestures operate the drone in right, left, right-rotate and left-rotate. The ranges of inner regions are defined as (-5° – -30°) and (+10° – +35°), while the range of the outer regions are (-90° – -30°) and (+35° – +90°). In addition, the normalized force spectrum from the threshold value of 0.2 to 1 drives the magnitude of drone movements with linear interpolation. The threshold value is designed to avoid unwanted activation. When the wrist angle falls into one of the eight regions, the user can mobilize the drone movement through exerting the right amount of force.

4 USER STUDY 1: UNIT TEST FOR DRONE MOVEMENTS

We conduct user studies to understand the user performance and acceptance of the four models mentioned above (Method 1 – 4, abbreviated as M1 – M4). We specifically focus on the first time the user is confronted with various combination of force-assisted interaction and IMU controls.

4.1 Participants and Apparatus

To understand the users' behaviour with the candidate gestures, we conduct a user study with 12 participants (18 - 27 years; 10 male and 2 female; all right-handed). All users were recruited from the university campus. All of them are experienced smartphone users. However, only three of them had prior experience of controlling a drone and only 1 of them had prior experience with force interaction.

We implement the four methods on an iPhone 7s Plus equipped with a pressure-sensitive touchscreen (5.5"). The touchscreen is responsive to pressures ranging continuously from 0 to 3.3 N, corresponding to 0 to 6.66 units in iOS (Swift) programming [83]. The smartphone is connected through WiFi to a consumer-grade drone (DJI Tello[5]) throughout the entire evaluation. Figure 2 shows the four testing interfaces. The two-handed method (Method 1) interface (Figure 2(a)) corresponds to the commonly used commercial interface for drone control. The user holds a smartphone in landscape mode with two hands. The left hand controls the horizontal and rotational movements while the right hand controls the lateral and longitudinal movements. The IMU-based interaction models (M2, M3 and M4) share the same single-button interface in portrait mode. The colour of the

[5]https://store.dji.com/shop/tello-series

button changes from dark grey (Figure 2(b)) to green (Figure 2(c)), once the users' wrist rotation exceeds the range in which the controls are supposed to take place. In M4, the button colour further varies with the wrist rotation from green in the inner region to red (Figure 2(d)) in the outer region. We encourage the users to focus on the drone movements, and employ their peripheral vision to receive the visual clues (i.e. the colour of the button). The smartphone also provides haptic clues for the force-assisted approaches (M3 and M4). In order to reduce the visual demands on the smartphone, the exerted force levels exceeding the normalized force spectrum of 0.2 and 0.75 respectively result in a single and a double vibration. Even though we draw a button at the bottom edge of the touchscreen, the users can perform an interaction outside the button area, which extends to the whole screen. The oval buttons allow the user to select the method, start the experiment, and send the logs to a computer connected to the same network. The interface also displays basic debug information such as Pitch, Roll, Yaw, Distance, Angle, and Force applied.

We informed participants that data will be de-identified, and all recorded data will be password protected and deleted after the study ends. Participants provided informed consent to participate in this study. The study was carried out following the General Data Protection Regulation (GDPR) and approved by university institutional ethics review board (IRB) regulations. The entire study, including all three experiments, was authorized by the IRB and occurred between May and October 2019.

4.2 Tasks

In this section, we only consider simple unit tests. We ask the participants to complete five operations for each method. Each run of the unit test consists of flying operations in a specific direction as follows: (1) horizontal upward movement (1.8 meters); (2) horizontal downward movement (1.8 meters); (3) right rotational movement (2 * 90°); (4) left rotational movement (2 * 90°); (5) Two-step rotational movement of 180° left rotation and 180° right rotation (no displacement);

When the two-button interface merges into a single button, additional modalities (IMU and force-sensitive interfaces) are introduced to handle the vertical and rotational movements. As joystick interfaces on the touchscreen for longitudinal and lateral movements are thoroughly investigated [72] for gaming and robotic scenarios, we focus on the user and drone interaction in horizontal and rotational movements. Besides, short and identical movements in a trial enable us to observe the user performance and behaviour during the drone control, and hence capture the users' wrist positions and movements for a given gesture. In contrast, multi-step and combinatorial movements represent a more complicated task. For instance, forward (horizontal) plus upward (vertical) movements will deteriorate the gesture footprints.

After showing the users the gestures and controls for a given interaction method, the participants have five minutes to get familiar with the interfaces and the gesture controls. A five-minute briefing session is sufficient as unit tests are straightforward and simple (e.g. last no longer than 10 seconds.) Every participant completes three trial of each unit test with each method. Three trials are sufficient because extended trials may lead to negative performance due to the task nature and accordingly boredom [56]. Among all trials, we record the completion time, touch behaviour, force exertion and IMU values. We provide cues in the tasks to make the drone movements in fair comparison, as follows. For horizontal movements, we define a ceiling and a floor (20 cm buffer distance from the actual ceiling and floor). Users can control the drone from the starting location (e.g. floor) to the ending location (e.g. ceiling). Regarding the rotational movements, the drone starts at the 0°, and, supported by the IMU embedded in the drone, the LED light on the drone will give visual cues to the users once the ending orientation has been reached. If the movements or rotations of the drones are mistakenly performed, we drop the trial and ask the participants to re-do the failed trial. It is important to note that the issues of over-shooting (e.g. location precision or orientation accuracy) are more relevant to the study of Fitts's Law [80] focusing on the difficulties of the drone operations with various controllers, while our study, in search of

Table 3. Results of completion time over five tasks with One-way ANOVA with Bonferroni and Holm Analysis: Italic numbers indicate no statistical significance between two pairs of methods.

Task	p-value	F-statics	DOF	M1 vs M2	M1 vs M3	M1 vs M4	M2 vs M3	M2 vs M4	M3 vs M4
1	2.91E-06	10.479	(3, 140)	*0.6047*	0.0181	2.00E-05	*0.0579*	8.94E-05	0.0795
2	7.77E-08	13.5981	(3, 140)	*0.1610*	0.0150	0.0002	0.0001	3.80E-06	*0.2963*
3	3.73E-07	12.2294	(3, 140)	0.0079	0.0006	1.25E-07	*0.4214*	0.0179	*0.0982*
4	6.66E-10	17.9276	(3, 140)	*0.0605*	0.0005	3.68E-10	*0.0808*	1.314E-05	0.0062
5	1.63E-5	9.0469	(3, 140)	*0.06001*	0.0244	4.67E-06	*0.5546*	0.0169	*0.0545*

subtle interactions on miniature interfaces, focuses on the observation of the user behavior among three modals. We instruct the users to complete the course as fast as possible for each trial. This instruction prevents the participants from operating the drone at extremely low speeds, which may sabotage the experiment's validity. For example, users with M2 can accomplish the task with very least wrist rotation and hence results in very low speeds but long completion times as a trade-off. We always start with the Two-handed method (M1). We then randomize the order of the remaining three methods (M2 – M4) in order to compensate for any asymmetric skill transfer [56] taking place during the experiment. We design this partial counterbalancing strategy with the following justifications. First, the flying drone is a moving object that may easily crash and hit the users or bystanders with an unfamiliar control interfaces . We consider that M1 is analogous to the two-handed tangible controllers that are the most common way to manipulate objects on smartphones and gaming consoles. M1 brings a reasonable level of user affordance [33], knowing that gestural inputs are indeed not completely natural [61]. Thus, choosing M1 as the starting method enables users to become familiar with the drone control in a physical reality [37]. Second, although full counterbalancing can alleviate the carry-over effect and hence reduce the internal validity [56], partial counterbalancing strategies have long been applied in within-subject evaluations [64]. For instance, Latin Square is a traditional strategy for partial counterbalancing, which is a good compromise but still poses carry-over effects [55]. That is, Latin Square has an inherited deficiency in which conditions precede and follow other conditions an unequal number of times. Due to the practical reality, it is difficult to achieve full randomization [25], while our scenario maintains a reasonable level of randomization. After all the trials, we distribute the NASA Task Load Index (NASA TLX) [36] questionnaires to collect the user perceptions with the four methods.

4.3 Results

4.3.1 Completion Time. Figure 3 shows the average completion times for each method. M3 and M4 are on average 16.54% and 27.86% faster than M1, while M4 is 22.19% faster than M2. It is important to note that the mean completion times of task (5) are at least twice more than that of the mean completion times of tasks (3) and (4) because of the doubled rotational degrees. Table 3 summarizes the statistical significance in completion times across the five tasks. One-way ANOVA shows that the interaction models has a significant effect on the completion time of all tasks. Bonferroni and Holm Analysis compare the statistical difference between two interaction models (column 5 – 10), where the number in italic format indicates no statistical difference in two interaction models. Methods 1 and 2 (M1 and M2) have no significant impact on four out of five tasks, while Methods 3 and 4 (M3 and M4) are significantly faster than M1 in all tasks. Similarly, M2 vs M3, as well as M3 vs M4, make no significant difference to the completion time (4 out of 5 tasks). However, M2 and M4 have significant effects on the completion time among all tasks. In other words, the statistical analysis implies that M3 and M4 are significantly faster than M1, and M4 is significantly faster than M2.

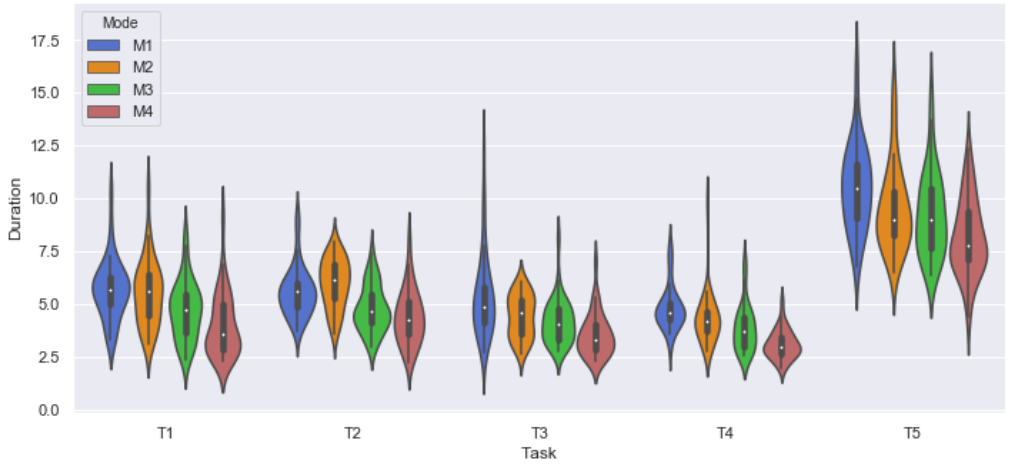

Fig. 3. Task completion time (M1 – M4). M3 and M4 have significantly shorter completion time than the commercial baseline (M1) (Checked the distribution normality with Kolmogorov–Smirnov Test).

4.3.2 Wrist Movements. Figure 4 shows the distributions of the users' Mean posture (M) and Movement degree (SD) of Row and Pitch in the five tasks. M1 relies solely on touch-based interactions on touchscreens. We thus neglect the IMU data of M1. M2, M3 and M4 and apply pitch gestures in tasks (1) and (2) as well as roll gestures in tasks (3) – (5), to maneuver the drone with vertical and rotational movements, respectively. Regarding the results, we rank the pitch gestures (T1 and T2) in ascending order: M3: 46.89° (+25.16° and -21.73°), M4: 70.93° (+44.33° and -26.60°), and M2: 84.10° (+40.30° and -43.81°), as well as the roll gestures (T3 and T4) in ascending order: M3: 49.19° (+29.74° and -19.46°), M4: 91.24° (+44.19° and -47.05°), and M2: 103.73° (+52.56° and -51.17°). Users with M2 performs the pitch and roll gestures through wrist movements. As the degree of wrist movements is linearly mapped with the magnitude of drone movements, the users turn their wrists to the maximum extent to shorten the task completion time. M3 manipulates the magnitude of drone movements through force levels. In this case, the users' wrists lean slightly towards the intended direction and control the force level with the thumb joints. Therefore, M3 results in wrist rotations 55.75% lower than M2. M4 serves as an intermediate solution between M2 and M3, which relies more on the wrist movement to establish a 2-level gesture. The gestures for longitudinal (forward and backward) and lateral (right and left) movements are performed within the inner wrist space, and the gestures for vertical (upward and downward) and rotational (right and left) movements within the outer region of the wrist rotation space (outer region). Therefore, the users tend to rotate their wrist to the outer region, where their average postures with M4 is close to M2. As a result, M4 requires 51.27% more wrist rotation than M3 as users find a confident angle in the outer region and exert the force accordingly. The wrist rotation of M4 is only 15.66% lower than M2 because M4 fully leverages the possible space of wrist rotation. M3 results in overall lower SD values for both the roll and pitch gestures. The key reason is that users only rotate their wrists over the threshold position and avoid extra wrist movements. In contrast, users with M2 and M4 experience higher SD values in the roll and pitch gestures as wrist rotations are vague on an imaginary interface even as visual clues are available.

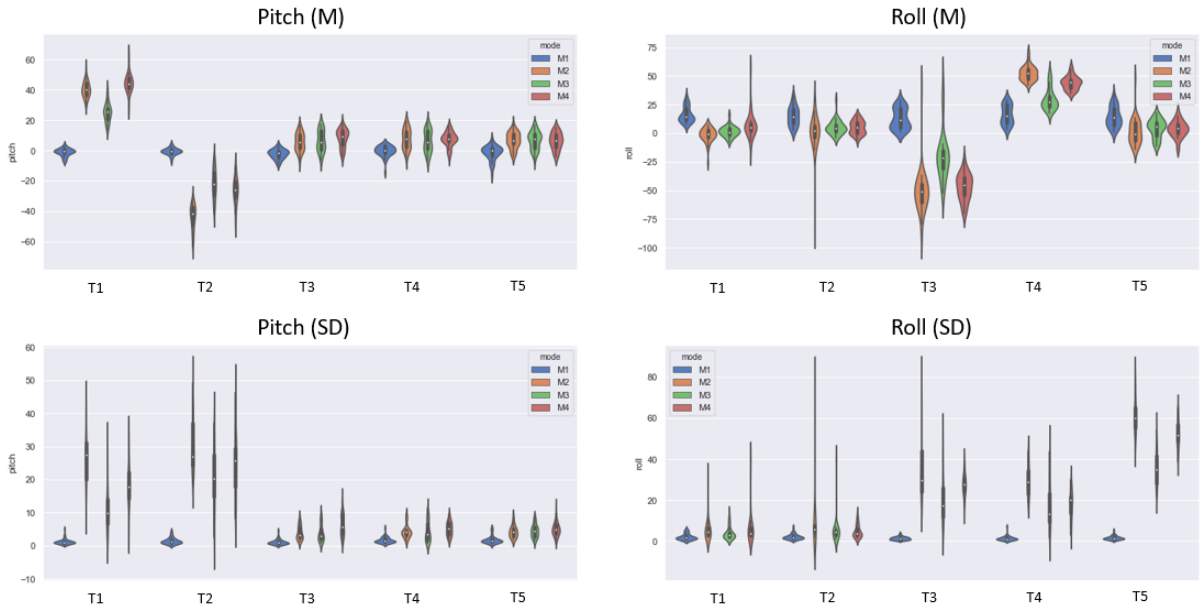

Fig. 4. Violin plots for Mean posture (M) and Movement degree (SD) of Row and Pitch (in degree °) across the five tasks (T1 - T5). Noted that M1 results SDs approximate to 0 due to the device holding position (Checked the distribution normality with Kolmogorov–Smirnov Test).

Table 4 shows the results of One-way ANOVA for the mean posture (M) and degree of movement (SD) with Yaw, Row and Pitch gestures. Almost all gestures across the five tasks (except Yaw-SD in the task (2)) show the statistical significance and thus we perform Bonferroni and Holm Analysis. Tables 5–9 lists the Holm p-value under the One-way ANOVA with Bonferroni and Holm Analysis.The six values at the right upper corner and the other six values at the left lower corner represent the statistical significance of the user's mean posture and movement degree, respectively. In general, Yaw gestures across the five tasks seldom show effects on the user's postures and movements, as the users perform randomized body orientation (left or right). In addition, M1 shows statistical significance in terms of row and pitch gestures across the five tasks, as the users hold the devices nearly parallel to the ground and other interaction methods follow the users' wrist angles. Among tasks (1) and (2) requiring Pitch gestures, the interaction models generate a significant difference to both the wrist posture and the movement degree. Among task (3) and (4) requiring Roll gestures, the interaction models has significant effects on both the wrist posture and movement degree. In task (5), roll gestures go bidirectionally to either left or right. Statistical significance exists in the wrist movement but not the wrist posture because the two discrete postures counterbalance the mean wrist posture.

4.3.3 Interaction Footprint. Figure 5 shows the interaction footprint for the four candidate methods. All figures show the displacement of the finger on an iPhone 7s Plus screen of size 414pt * 736pt. We combine the movements of all 12 participants across the five tasks in these figures and we capture one sample every 10 ms. We calculate the interaction area by first finding the centre of the captured samples; We then compute the standard deviation on each axis. The interaction area corresponds to three times the standard deviation from the centre (99.7% of the samples). If the calculated interaction area exceeds the screen boundaries, we consider the screen edges as the interaction area boundary for the considered edge. Among the five tasks, only the left-hand button in M1 is

Table 4. One-way ANOVA analysis for Mean posture (M) and Movement degree (SD) across the five tasks: At the degree of freedom (3, 140) and Italic numbers indicate no statistical significance

Task	**T1**		**T2**		**T3**		**T4**		**T5**	
Gesture	**p-value**	**F-statics**	**p-value**	**F-statics**	**p-value**	**F-statics**	**p-value**	**F-statics**	**p-value**	**F-statics**
Yaw-M	0.0098	3.9432	1.27E-09	17.327	4.35E-09	16.1869	1.11E-16	42.4356	1.11E-16	37.599
Yaw-SD	0.0208	3.3548	*0.0694*	2.4121	0.0102	3.9078	9.05E-11	19.8289	0.0070	4.2045
Row-M	1.11E-06	36.6339	2.77E-07	12.4853	1.11E-16	116.3431	1.11E-16	15.5432	3.01E-08	14.4375
Row-SD	0.0017	5.3337	0.0001	7.5368	1.11E-16	75.7482	1.11E-16	80.9359	1.11E-16	493.5574
Pitch-M	1.11E-06	528.5515	1.11E-16	181.1792	1.09E-12	24.2297	8.11E-09	15.6192	5.84E-11	20.2538
Pitch-SD	1.11E-06	113.1824	1.11E-16	91.7556	3.22E-14	27.9319	1.91E-09	16.9466	3.43E-12	23.0619

Table 5. One-way ANOVA with Bonferroni and Holm Analysis for Mean posture (right upper corner) and Movement degree (left lower corner) for Task 1: Italic numbers indicate no statistical significance between two pairs of methods (M1 – M4)

Yaw	**M1**	**M2**	**M3**	**M4**	**Row**	**M1**	**M2**	**M3**	**M4**	**Pitch**	**M1**	**M2**	**M3**	**M4**
M1	-	*0.7507*	*0.8515*	0.0130	**M1**	-	0	1.33E-12	1.62E-06	**M1**	-	0	0	0
M2	*0.4938*	-	*0.9000*	0.0290	**M2**	0.0047	-	*0.0918*	4.93E-05	**M2**	0	-	0	0.0018
M3	*0.7919*	*0.5185*	-	*0.1700*	**M3**	*0.3387*	*0.1668*	-	0.0129	**M3**	2.47E-10	0	-	0
M4	0.0308	*0.6016*	*0.0547*	-	**M4**	0.0070	*0.8495*	*0.1927*	-	**M4**	0	5.63E-08	3.34E-06	-

Table 6. One-way ANOVA with Bonferroni and Holm Analysis for Mean posture (right upper corner) and Movement degree (left lower corner) for Task 2: Italic numbers indicate no statistical significance between two pairs of methods (M1 – M4)

Yaw	**M1**	**M2**	**M3**	**M4**	**Row**	**M1**	**M2**	**M3**	**M4**	**Pitch**	**M1**	**M2**	**M3**	**M4**
M1	-	4.89E-06	1.24E-05	1.24E-09	**M1**	-	1.32E-07	0.0004	0.0004	**M1**	-	0	0	0
M2	*0.1267*	-	*0.7928*	0.1700	**M2**	6.42E-05	-	*0.1191*	*0.1682*	**M2**	0	-	0	8.88E-06
M3	*0.8697*	*0.4945*	-	*0.1430*	**M3**	*0.4786*	0.0079	-	*0.9786*	**M3**	0	7.02E-07	-	0.0102
M4	*0.2006*	*0.7949*	*0.5990*	-	**M4**	0.395	0.0067	*0.9052*	-	**M4**	0	0.0006	*0.0837*	-

Table 7. One-way ANOVA with Bonferroni and Holm Analysis for Mean posture (right upper corner) and Movement degree (left lower corner) for Task 3: Italic numbers indicate no statistical significance between two pairs of methods (M1 – M4)

Yaw	**M1**	**M2**	**M3**	**M4**	**Row**	**M1**	**M2**	**M3**	**M4**	**Pitch**	**M1**	**M2**	**M3**	**M4**
M1	-	4.38E-05	3.65E-06	5.66E-09	**M1**	-	0	3.06E-13	0	**M1**	-	8.78E-08	5.94E-09	5.52E-12
M2	*1.2889*	-	*0.5327*	*0.1417*	**M2**	0	-	4.44E-13	*0.2889*	**M2**	6.32E-06	-	*0.5600*	*0.1686*
M3	*1.1371*	*0.8257*	-	*0.3418*	**M3**	7.89E-12	1.38E-09	-	1.01E-10	**M3**	1.21E-05	*0.8429*	-	*0.3640*
M4	0.0113	*0.0752*	*0.0519*	-	**M4**	0	0.0012	0.0017	-	**M4**	4.00E-15	0.0002	0.0001	-

Table 8. One-way ANOVA with Bonferroni and Holm Analysis for Mean posture (right upper corner) and Movement degree (left lower corner) for Task 4: Italic numbers indicate no statistical significance between two pairs of methods (M1 – M4)

Yaw	**M1**	**M2**	**M3**	**M4**	**Row**	**M1**	**M2**	**M3**	**M4**	**Pitch**	**M1**	**M2**	**M3**	**M4**
M1	-	3.40E-11	6.88E-14	0	**M1**	-	0	1.84E-11	0	**M1**	-	1.35E-07	1.43E-05	2.61E-07
M2	1.75E-11	-	*0.2509*	0.008	**M2**	0	-	0	8.64E-06	**M2**	6.33E-05	-	*0.8150*	*0.8621*
M3	6.58E-05	0.0053	-	*0.1171*	**M3**	2.66E-14	1.18E-09	-	1.38E-12	**M3**	7.14E-06	*0.9816*	-	*0.7083*
M4	5.72E-05	0.0047	*0.9299*	-	**M4**	1.11E-15	1.26E-08	*0.5869*	-	**M4**	2.38E-09	*0.2641*	*0.1847*	-

Table 9. One-way ANOVA with Bonferroni and Holm Analysis for Mean posture (right upper corner) and Movement degree (left lower corner) for Task 5: Italic numbers indicate no statistical significance between two pairs of methods (M1 – M4)

Yaw	M1	M2	M3	M4	Row	M1	M2	M3	M4	Pitch	M1	M2	M3	M4
M1	-	1.20E-14	6.33E-13	2.00E-14	**M1**	-	9.30E-08	2.06E-05	6.96E-06	**1**		6.80E-09	1.11E-08	3.16E-08
M2	*1.0885*	-	*1.3431*	*0.9087*	**M2**	0	-	*0.624*	*0.6744*	**M2**	1.79E-07		*0.8954*	*2.1012*
M3	*1.1268*	*0.7391*	-	*1.038*	**M3**	0	0	-	*0.7631*	**M3**	1.97E-08	*0.6214*		*1.5999*
M4	0.0074	*0.0738*	*0.0370*	-	**M4**	0	5.33E-07	*0*	-	**M4**	1.28E-11	*0.1702*	*0.3120*	

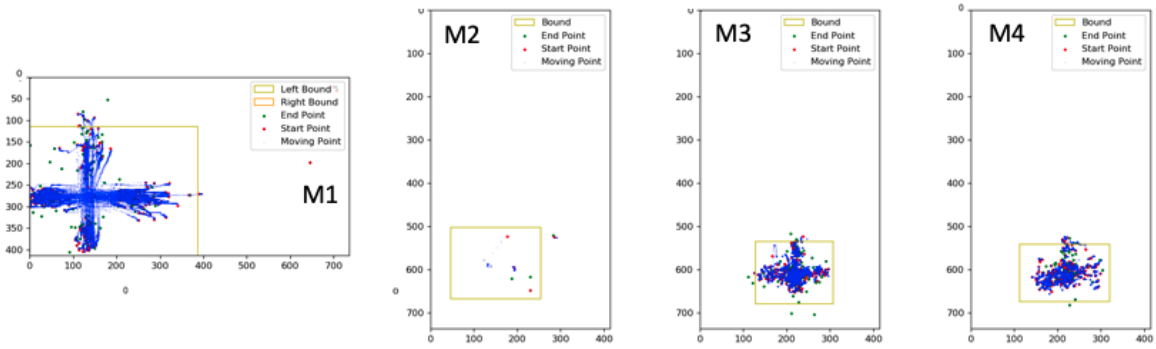

Fig. 5. On-screen interaction footprint for all four methods (M1 – M4) for the 12 participants. M3 results in the lowest footprint, closely followed by M4. The solely touch-based interface (M1) requires using most of the screen for interaction.

used for the horizontal and rotational movements, and hence touch-points on the right-hand button are rarely spotted. The interaction area of the left-hand button in M1 is 160,970 pt^2 and occupies 52.83% of the screen. In comparison, users with M2 solely rely on wrist rotations, primarily roll and pitch gestures, to drive the drone movements rotationally and horizontally. However, some touchpoints are recorded because users are used to putting their thumbs on the button interface. As a result, the IMU-induced method (M2) results in an interaction area of 34,365 pt^2, equivalently to 11.28% of the screen. Both M3 and M4 require users to touch the screen to exert force, which leads to interaction areas of 25,874 pt^2 and 27,460 pt^2, occupying 8.49% and 9.01% of the screen, respectively. The additional modalities of IMU and force-assisted input not only liberate one hand of the user but also significantly save the interaction space by 41.55% – 44.34% compared to the two-handed method. M3 results in a slightly smaller (5.77% less) and denser footprint (σ_x = 29.88 and σ_y= 24.06) than M4 (σ_x = 35.13 and σ_y= 22.11). Even though both M3 and M4 employ the force spectrum to adjust the magnitude of the drone movements, the difference in footprint is mainly caused by the wrist movements. That is, as the thumb and wrist muscles are interconnected, they pose ergonomic constraints. The users with M4 re-adjust their thumbs into a comfortable position for easier force exertion, especially when the users' wrists are approaching their maximum extents within the outer regions of drone movements in horizontal and rotational directions.

4.3.4 User Experience and NASA TLX Survey. One-way ANOVA reveals no significant effects on all the metrics: 1) Mental ($F_{(3,44)}$ = 0.2123, p = 0.8874), 2) Physical ($F_{(3,44)}$ = 0.2886, p = 0.8334); 3) Temporal ($F_{(3,44)}$ = 0.3898, p = 0.7609); 4) Performance ($F_{(3,44)}$ = 1.7872, p = 0.1635); 5) Effort ($F_{(3,44)}$ = 0.5542, p = 0.6481) and 6) Frustration ($F_{(3,44)}$ = 0.5350, p = 0.660753). Unit tests are indeed too short for participants to clearly distinguish the demands

between the methods with the unit tasks. Longer testing sessions with more complex tasks would be required in order to see a shift in user experience.

4.4 Discussion

When the human-to-drone input significantly shrinks from two-handed buttons to a single-handed interface, additional modalities can augment the input options within a constrained space. The five unit tasks shed light on the design of drone control with multi-modal inputs including touch-based, IMU-induced and force-assisted interactions. The two-handed buttons (M1), as a commercial baseline, emulate joystick controllers and rely solely on touch-based interactions (left button: horizontal and rotational movements; right button: lateral and longitudinal movements). M2 and M3 feature a single touch-based button for lateral and longitudinal movements, while IMU-induced movements in M2 and force-assisted thumb interaction in M3 drive the horizontal and rotational movements. Finally, M4 applies force-assisted interaction for the magnitude of drone movements, and further divides the pitch and roll gestures into a 2-level IMU region. The inner region of wrist rotation maps the drone in lateral and longitudinal directions, while the outer region of wrist rotation manipulates the drone horizontal and rotational movements.

In other words, M1, M2, and M3 share the same interface for lateral and longitudinal movements. Horizontal and rotational drone movements are governed by various combinations of modalities among all interaction methods. To make a comparable observation, we focus on user behaviour with the horizontal and rotational movements. In search of an effective yet subtle interaction approach within the thumb-to-finger space interaction, we consider the candidate models according to the completion time, wrist movements and interaction areas. Regarding the completion time, M3 and M4 are both effective solutions, outperforming M1 significantly. Surprisingly, M2 is only slightly better than M1 without statistical significance, even though we already optimized M2 and neglect another inferior alternative approach similar to the pen-based Nintendo Wii controller[6]. To perform the pitch and roll gestures for the drone movements in the horizontal and rotational directions, M2 and M4 both require at least 51.27% more wrist rotation than M3. In M4, as the inner region of wrist rotation substitutes the touch-based interaction, the users, in order to avoid confusing inputs, tend to rotate their wrist closer to their maximum extents, leading to mean angles similar to M2. The NASA TLX questionnaire does not show a significant difference in user acceptance between interaction models (M1 – M4). The majority of participants (7 out of 12) reflected that M4 is unnatural and counter-intuitive when multiple flying operations are involved. For example, the drone in task 5 requires both left and right rotations, for which users need to perform two roll gestures in two disconnected outer regions. Accordingly, they usually release their thumbs when their wrists traverse the inner region to avoid unwanted operations. Even though M4 is slightly faster than M3 (without statistical significance in 4 out of 5 tasks), we do not consider M4 in further stages. Considering M3 results in short completion times (Section 4.3.3) with the least wrist rotation, we select M3 as the interaction method for our ring device. Finally, all methods (M1 – M4) are robust in the tasks, as the users rarely failed a trial, where the total counts of the failed trials in the five tasks are 19 (4 (M1), 5 (M2), 4 (M3), 6 (M4)) out of 720 trails (12 participants * 5 tasks * 3 trials in each task * 4 methods).

We noticed two core limitations. First, this user study neglects the drone controls in lateral and longitudinal directions. As the ultimate goal of this paper is to design a drone controlling device with thumb-based interaction within the finger space, we design an additional task involving lateral and longitudinal directions in the next section. The task will allow us to have a more comprehensive understanding of the interaction area involving all flying operations, and figure out the perceived task demands in a more complicated flying route. Second, one may argue that our partial counterbalancing strategy poses the carry-over effect [55] and hence internal validity [56], which implies that the first method being tested, M1, is less advantageous than others. However, M1,

[6] http://people.cs.vt.edu/ bowman/3dui.org/course$_n$otes/chi2009/wiimote.pdf

as the commercial standard, serves as the baseline in this study. Users with M1 could get additional performance improvements due to prior experience from the game console on smartphones or even two-handed tangible controllers. Therefore, it is hard to justify whether the completion time will increase or decrease. Regarding the results of wrist movements and interaction areas, we can obviously see that M1 does not rely on the IMU-driven interaction and our partial counterbalancing strategy preserves the validity of our findings.

5 USER STUDY 2: 8-SHAPE FLYING MOVEMENTS

In this test, we investigate the interaction area and the users' perceived task load in a more complicated scenario. In the first study, the users did not perform lateral and longitudinal movements and the touch behaviours are not truly reflected, i.e., the right-hand-side button of M1 and the touch-based interaction of M2 are missing. Besides, users cannot perceive task load differences between the proposed methods with unit tests in Section 4.3.4.

5.1 Participants, Apparatus and Tasks

To understand the users' behaviour with the candidate gestures, we conduct a user study with another 20 participants (20 - 33 years; 17 male and 3 female; all right-handed). All users were recruited from the university campus and all of them are experienced smartphone users. However, only four of them had prior experience with controlling a drone, and three of them had prior experience with force interaction.

We implement the four methods on an iPhone 7s Plus equipped with a pressure-sensitive touchscreen (5.5"). The touchscreen is responsive to pressures ranging continuously from 0 to 3.3 N, corresponding to 0 to 6.66 units in iOS (Swift) programming [83]. The smartphone is wirelessly connected to a consumer-grade flying drone (DJI Tello[7] throughout the entire evaluation. We use the same interface as in the previous experiment (Figure 2(a) – (c)) for M1 – M3. We ask the participants to complete three trials of a figure-8 flying route with the three methods. In each trial, the user controls the drone to draw a figure-8 route around two identical obstacles. Both obstacles are 160 cm * 110 cm and are separated by a distance of 640 cm. As the flying drone only makes an approximate 8-shape path in a spacious room, no failing trials are counted in the user study. The users have to apply longitudinal, lateral and rotational drone movements to accomplish the task. After demonstrating to the users the controls for a given method, we give the participants five minutes to get familiar with the interfaces and the gesture controls. Similarly, a five-minute briefing session is sufficient because unit tests are straightforward and simple, and last no longer than 10 seconds. Each participant completes three trials with each method. We record the touch behaviours among all trials and we instruct the users to complete the course as fast as possible for each trial. We start with the Two-handed method and the justifications are explained in the previous section. We then randomize the order of the next two methods in order to compensate for any learning effect taking place during the experiment. After all the trials, the questionnaires of NASA Task Load Index (NASA TLX) [36] were distributed to collect the user perceptions with the four methods. As stated in Section 4.1, in additional to the participant's consent, the collected information from the evaluation was out following the General Data Protection Regulation (GDPR) and approved by university IRB regulations.

5.2 Results

5.2.1 Interaction Footprint. Figure 6 shows the interaction footprint for the touch-based method (M1), IMU-induced method (M2) and force-assisted method (M3). All figures show the combined displacement of the finger for all 20 participants on an iPhone 7s Plus screen of 414pt x 736pt. We capture one sample every 10 ms and we calculate the interaction area by first finding the centre of the captured samples. We then compute the standard deviation on each axis. The interaction area corresponds to three times the standard deviation from the centre (99.7% of the samples). If the calculated interaction area exceeds the screen boundaries, we consider the screen

[7]https://store.dji.com/shop/tello-series

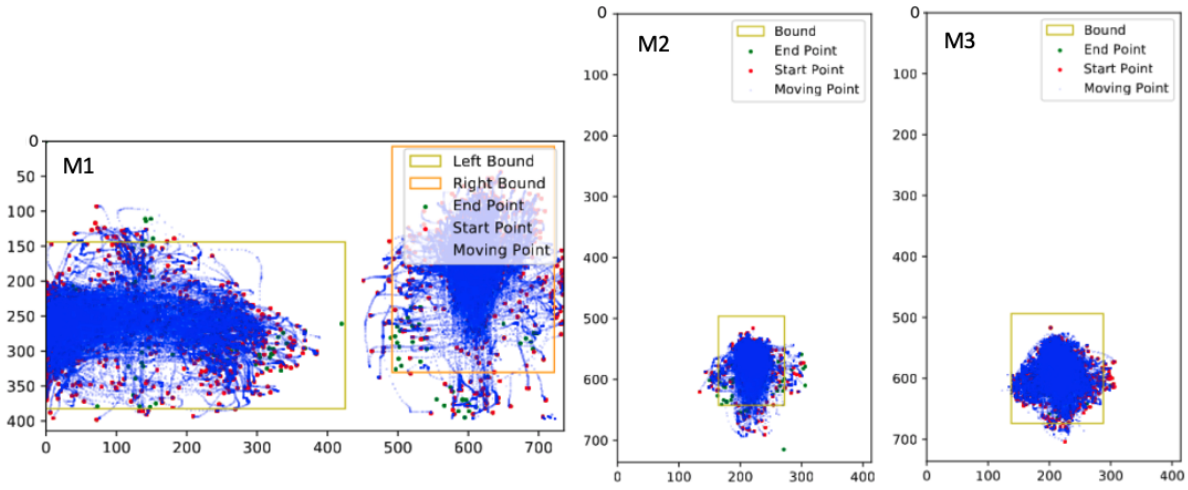

Fig. 6. The on-screen interaction footprint for all three methods for 20 participants. The force-assisted method (M3) results in the lowest footprint, closely followed by the IMU method. The two-handed method requires the use of most of the screen for interaction.

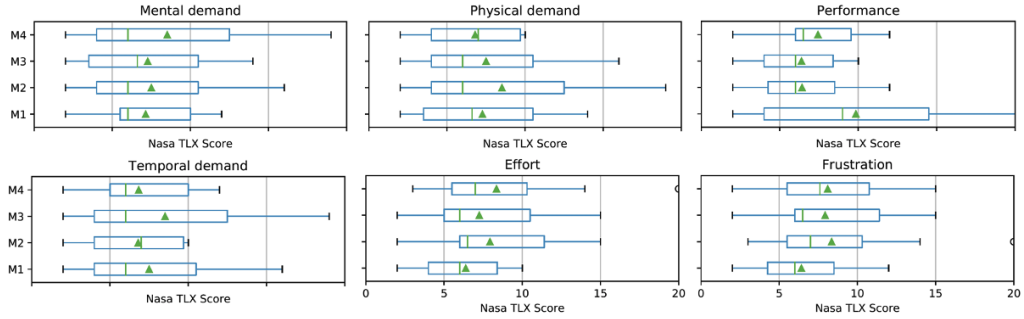

Fig. 7. NASA TLX Results for the three methods: Two-Handed touch-based (M1), IMU-induced (M2) and Force-assisted (M3) interactions.

edges as the interaction area boundary for the considered edge. The two-handed method produces two separate interaction areas of respective 143,795 pt^2 (left) and 74,442 pt^2 (right). The combined interaction areas occupy 71.6% of the screen. In comparison, the Force touch method and the IMU method respectively result in an area of size 15,741 pt^2 and 27,055 pt^2, occupying 5.2% and 8.9% of the screen. Once again, the new modality of force and wrist movement not only free up the users' hand but they also save respectively 66.4% and 62.7% of the screen real-estate compared to the two-handed method. M2 has a significantly smaller (41.6% less) and denser footprint than M3. We may explain this observation by the fact that the IMU method is more intuitive for untrained users during a more complicated task. Indeed, we rarely employ force-assisted interaction in our daily routines. As such, participants may be more precise in their interaction when using the IMU method, thus requiring less correction and fewer movements.

5.2.2 User Experience and NASA TLX Survey. We then distributed standard NASA TLX survey forms [36] to the participants at the end of the experiment session. Figure 7 presents the results of the survey. On average, for all parameters, users report the lowest scores for the IMU-induced method (M2), followed by the force-assisted method (M3), and finally the two-handed method (M1). The M2 is the only method resulting in scores below 10/20 for the physical demand (9.8), temporal demand (9.5), effort (9.3), and frustration (8.2). However, each method displays a high variance in the results reported by the users. One-way ANOVA shows a barely statistically significant effect of the techniques ($p<0.05$) for all parameters except Physical Demand ($p=0.1237$). The Bonferroni and Holm pairwise comparisons show no significant differences between M1 and M3 ($p>0.5$ for all criteria). Similarly, there is no significant difference between M2 and M3 for all criteria ($p>0.5$). However, the Bonferroni and Holm method displays a significant difference between M1 and M2 for the Mental Demand ($p<0.05$), Temporal Demand ($p<0.05$), Performance ($p<0.05$), Effort ($p<0.05$), and Frustration ($p<0.05$). Overall, the M3 results in a lower reported load than M1. Although M3 does not result in being statistically different to M1, it frees one of the hands of the user, allowing the control in other devices such as smartwatches or smart rings, without resulting in a loss of usability.

6 SYSTEM AND HARDWARE IMPLEMENTATION

The second user study shows evidence that the IMU-induced interaction (M2) has a smaller interaction area than the force-assisted interaction M3. M2 and M3 respectively occupy 5.2% and 8.9% of the iPhone touchscreen (12.18 x 6.85 cm^2). As such, M2 and M3 need rectangle shaped areas of (0.63 * 0.36 cm^2) and (1.08 * 0.61 cm^2), respectively. This difference in size is not significant to the physical form factor because a ring-form device can comfortably accommodate such small areas. Regarding the user perceived load, M3 scores between M1 and M2 with no significant statistical significance between them. However, M2 presents completion times similar to the commercial baseline M1. Meanwhile, M3 results in a significantly shorter time than M2 and M1, allowing more subtle wrist movements for one-handed interaction. Considering the results in a holistic way, M3 is an effective and subtle solution with acceptable user feedback within a reasonably-sized interaction area. This section describes the implementation of M3 within a prototypical ring hardware system, and the form factor of the proof-of-concept device and interface.

6.1 System Description

Our prototype system takes the form of a force-sensitive ring. The architecture of the system is centred around a `Arduino Uno` that interfaces the various embedded sensors. The ring embeds an `IMS054-C04` pressure sensor and an `MPU9250` Inertial Measurement Unit (IMU). The pressure sensor can measure forces up to 2 kg (19.6 N). The Arduino Uno gathers information from the sensors, and forwards the corresponding instructions via an `HC05` Bluetooth module. Although most drones, including our demonstration drone, rely on WiFi for transmission, we use Bluetooth for our system. Bluetooth displays much lower energy consumption, which is a critical factor in extremely size-constrained devices such as smart rings. We communicate with the drone through an intermediate laptop, that transparently forwards the instructions coming via Bluetooth from the ring to the drone's WiFi interface. Figure 8 displays the hardware between our prototype interface.

We place the pressure sensor on top of the IMU on the side of the user's index finger closest to the thumb (left side for right-handed users, and right side for left-handed users). The user can control the speed of the drone using the pressure sensor. The sensor can measure pressures between 0 and 2 kg that correspond to values between 0 and 1024 after analogue-to-digital conversion in the Arduino. The first user experiment (Section 4) revealed that users could not finely control pressures under 250 g. As such, we only consider values between 256 (500 g) and 1024 (2 kg). The drone model we are using takes values between 1 and 100 and converts them into three discrete speeds. We normalize the measured values to that scale and transmit them directly to the drone.

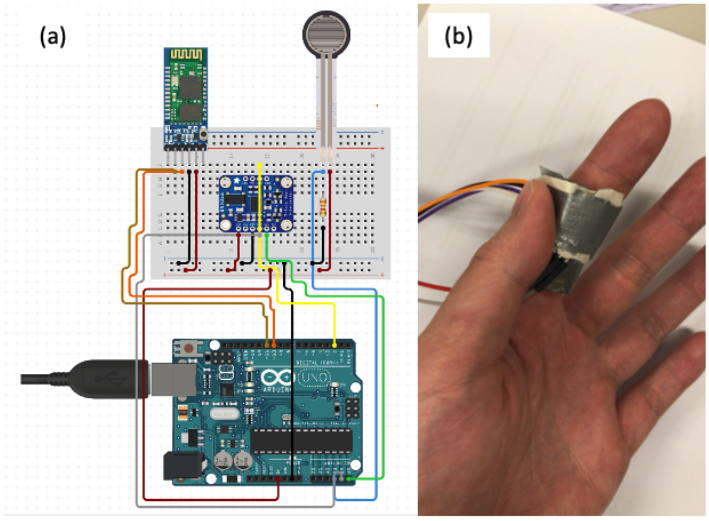

Fig. 8. Pitch and roll operations on our prototype system. (a) Schematics of our prototype system; (b) Our prototype system in action.

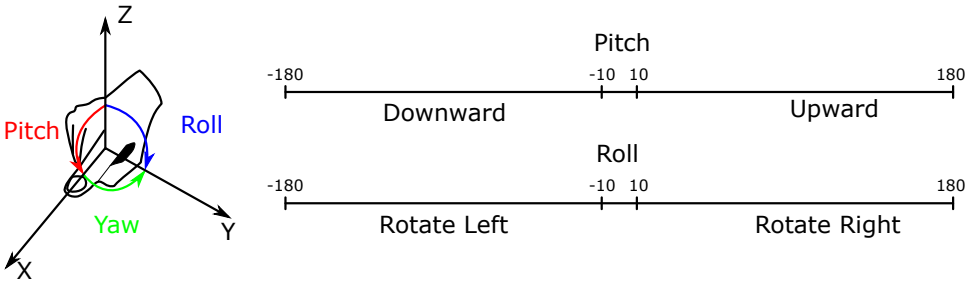

Fig. 9. Pitch and roll operations on our prototype system.

According to our measurements, the drone's speed adapts according to the following pattern: $[500\,g - 800\,g]$ results in the lowest speed, $[800\,g - 1250\,g]$ results in the medium speed, and $> 1250\,g$ results in the highest speed. We directly match the measured pressure to the drone speed, with minimum and maximum pressures (corresponding to the minimum and maximum speeds) as 0.25 (500 g) and 1 (2 kg), respectively. The user controls the drone movement using the IMU. We summarize the IMU operations in Figure 9. An IMU can measure three parameters: pitch (top of the finger pointing up or down), roll (rotation of the finger left or right parallel to the X-axis), and yaw (rotation of the finger left or right perpendicular to the Z-axis), represented as a value between 0 and 180°. In this study, we only consider the pitch and roll of the IMU. We establish a safety zone between -10° and +10° in which the drone does not move in horizontal and rotational directions. When the pitch reaches more than +10°, the drone moves upward, while the drone moves downward when the pitch value is below -10°. Similarly, the roll gesture rotates the drone once the wrist angle exceeds the threshold values of +10 (right-rotation) and -10 (left rotation).

6.2 Limitations and Potential Improvement Areas of the Prototype Design

The prototype system we developed is bulky and cumbersome to use as a wireless ring in a real-world setting. However, only a few modifications are necessary to turn this simple proof-of-concept into a fully-functional, independent ring for one-thumb drone control:

- Downsize the Arduino microcontroller. The Arduino Uno we are using embeds an ATmega328P, which, although powerful, takes up a relatively large space (37.4 x 6.76 mm) on the board, has a relatively high power consumption (12 to 16mA), and features many unnecessary inputs and outputs. Comparatively, a smaller chip such as an ATtiny85 (SOIC format) is only 5.4x5.4 mm, features more than enough power for our operations, and can consume less than 2mA.
- Similarly to the main microcontroller chip, we can downsize the Bluetooth and the IMU modules, and integrate them within the same circuit board. This would us allow to significantly reduce the size of the system by compacting all the active elements within a single board smaller than 2x2 cm.
- Add a battery for autonomous operation. A 50mAh battery is less than 2x1 cm, and can power the entire system for several hours.
- Use a smartphone instead of a laptop for transferring instructions from the Bluetooth interface to the WiFi interface.

The above modifications would still lead to a relatively bulky (2x2 cm interaction surface), yet fully autonomous and usable ring, with an acceptable autonomy. By further downsizing the components and adapting to a ring form factor, we expect to be able to integrate all the components within a 7mm wide, 3mm thick ring, similar to currently available commercial smart rings (For instance Mymotiv[8])

6.3 Feasibility Study of the prototype

In order to validate the effects of additional modalities applied to the proof-of-concept device, we set up the following experiment: we invite the 12 participants from the 1st user study (Section 4) to perform five unit tests (identical to the five tasks (T1 – T5) in Section 4). After the briefing session about the controls, the participants go through a 5 minutes acclimation phase during which they freely control the drone with our hardware device freely. The five-minute session is sufficient as we aim to capture the true user behaviors without over-training. After the tests, we conduct a survey on technology acceptance with the users. We ask the users to rate their technological literacy on a five-point likert scale ranging from 1 to 5, 5 being the highest. The average technological literacy is high, 3.70, ranging from 3 to 5. Through this survey, we aim at measuring the following constructs: Perceived Usefulness (PU), Perceived Ease Of Use (PEOU), and Intention Of Use (IOU). We also calculate the Cronbach Alpha reliability coefficient for the three constructs. For all three measurements, a coefficient above 0.70 denotes an acceptable consistency in the results. We compute the three coefficients for PU, PEOU and IOU, as shown in Table 11. As stated in Section 4.1, in addition to the participant's consent, the collected information from the evaluation was out following the General Data Protection Regulation (GDPR) and is approved by the university IRB regulations.

6.3.1 Completion Time. We compare the performance of the on-finger device with M3 in Section 4. Among T1 – T4, the participants achieve shorter completion times than M3 by 30.24% – 50.46%. In the multi-step task (T5), the participants also improve by 27.99%. The critical reason for the improvement in speed is the reduced load on the users' hand. Instead of holding a smartphone (M3 in Section 4), users hold a natural hand posture with a light-weight on-finger device facilitating faster wrist rotation and hence, shorter completion time.

One-way ANOVA shows the interfaces give statistical significance to the completion time among all tasks: T1 – ($F_{(1,70)}$ = 23.1918, p<0.01); T2 – ($F_{(1,70)}$ = 63.2173, p<0.01); T3 – ($F_{(1,70)}$ = 24.8668, p<0.01); T4 – ($F_{(1,70)}$ = 20.1934,

[8] https://mymotiv.com/the-ring/

Table 10. The Wrist Postures (Pitch and Roll) with the prototype and their statistics values for the hardware device (F: F-statics; $\bar{M}_{HW}$: mean wrist posture; σ_{HW}: standard deviation of wrist rotation) among the five tasks.

Task	**Pitch**				**Roll**			
	p-value	F	$\bar{M}_{HW}$	σ_{HW}	**p-value**	F	$\bar{M}_{HW}$	σ_{HW}
1	0.1686	1.93	+19.08	25.49	0.3486	0.89	5.30	23.44
2	0.3667	0.83	-24.16	12.65	0.0069	7.75	-2.54	15.02
3	5.82E-05	18.32	-2.80	10.90	0.8502	0.04	-18.26	30.85
4	1.21E-04	16.59	-1.67	9.15	0.6883	0.16	28.09	22.60
5	7.42E-04	12.45	0.33	8.94	0.0485	4.03	-1.84	16.52

p<0.01); T5 – ($F_{(1,70)}$ = 32.4981, p<0.01). The tasks show mean the completion times (in second) with the standard deviation values as follow: T1 – ($\bar{M}_1$ = 3.30, σ_1 =1.07); T2 – ($\bar{M}_2$ = 3.18, σ_2 =0.51); T3 – ($\bar{M}_3$ = 3.19, σ_3 =0.46); T4 – ($\bar{M}_4$ = 2.91, σ_4 =0.57); T5 – ($\bar{M}_5$ = 7.22, σ_5 =0.70).

6.3.2 Wrist Postures with Pitch and Roll. We compare the average wrist posture with findings of M3 with a smartphone (Section 4). Table 10 lists the analysis with One-way ANOVA showing the effects of form factor (smartphone vs on-finger device). No statistical significance to the form factor exists, in terms of Pitch gesture (Task 1 and 2) as well as Roll gesture (Task 3 and 4). As Task 5 applies roll gestures for both left and right drone rotations, we neglect the counteracted wrist angles. The participants with M3 on a smartphone achieve a small wrist range of 46.89° (+25.16° and -21.73°) and 49.19° (+29.74° and -19.46°) for pitch and roll gesture, while the participants with the prototype device display slightly smaller wrist posture of 43.24° (pitch: +19.08° and -24.16°) and 46.35° (roll: +28.09 and -18.26), respectively. The consistent wrist postures imply that users with different device tend to perform subtle wrist movements with the selected method.

6.3.3 Technology Acceptance. At the end of the user experiment, we distribute a Technology Acceptance Survey questionnaire among the participants. The questions and the results from the survey are presented in Table 11. We ask the participants to rate each sentence on a 1-5 points likert scale, with 1 being "totally disagree" and 5 "totally agree". Overall, the participants are particularly positive. They found the prototype device to be easy to use ($\bar{M}$ = 3.58, σ = 1.16), solving one of the major concerns raised by the participants of the first experiment. Indeed, using the traditional joystick was reported to be less ubiquitous. Participants also considered the prototype device easy to learn ($\bar{M}$ = 3.58, σ = 1.16) and became skillful ($\bar{M}$ = 3.33, σ = 0.78). No one scored less than 2 for any of the items in the PEOU. The participants also considered the prototype to be a convenient solution to control the drone ($\bar{M}$ = 3.08, σ = 1.08). Although they considered that using the prototype would only be a slight improvement in the way they control the drone over a traditional joystick controller ($\bar{M}$ = 3.25, σ = 1.36), they found the prototype useful ($\bar{M}$ = 3.67, σ = 1.07), especially for a mobile scenario ($\bar{M}$ = 3.92, σ = 1.44). Finally, users generally agree with using the ring-form prototype in the future, either alone, or as a complement to conventional joystick controllers, and they agree they would use it frequently. Overall, the Perceived Ease Of Use is positive with our prototype, achieving our goal of making a convenient interface for drone controls. Although PU and PEOU show higher variance values, the overall response to our ring-form prototype is consistently positive.

6.4 Discussion

6.4.1 Performance. Most of the recent works on controlling drones focus on proving the feasibility of natural interfaces for drone controls without showing quantitative results from experiments, including gaze [31], body movements [60], sitting angle [40], mind [45, 62], and speech [48]. Alternatively, other works elicit the user acceptance of the proposed control gestures [63], and consider user opinions such as 'how fun/reliable/easy

Table 11. Technology Acceptance Survey. The PU, PEOU and IU Score Higher than Average.

Question	AVG	MED	MIN	MAX	STDEV	95%CONF
Perceived Usefulness (PU), $\alpha = 0.7563$						
Using the device would enable me to control a drone more conveniently.	3.08	3	1	5	1.08	0.61
Using the device would improve the way I control a drone.	3.25	3	2	5	1.36	0.77
I would find the device useful when controlling a drone.	3.67	4	2	5	1.07	0.61
I find the device useful for controlling a drone with high mobility.	3.92	3.5	2	5	1.44	0.82
Perceived Ease Of Use (PEOU), $\alpha = 0.7187$						
Learning to use the device would be easy.	3.58	3	2	5	1.16	0.66
I would find it easy to get the device to control the drone.	3.67	3.5	2	5	1.15	0.65
I would become skillful at using the device.	3.33	4	2	5	0.78	0.44
I find the device easy-to-use.	3.58	4	2	5	1.16	0.66
Intention Of Use (IOU), $\alpha = 0.887$						
When the device becomes available, I intend to use it for controlling the drone.	3.25	3	2	4	0.62	0.35
When the device becomes available, I will use it in parallel to a joystick controller.	3.50	4	2	5	0.90	0.51
When the device becomes available, I predict I would use it frequently.	3.50	3.5	3	4	0.52	0.30

was the method' [31]. As the task completion time depends primarily on the drone's motor speed and moving distance, it is hard to compare the results without reporting the drone moving's distance in their tasks [44]. Thus, we focus our discussion on the following two dimensions: (1) the promptness and (2) the subtlety of the gestures. Regarding the promptness of the gestures, a two-handed gestural system [63] results in users spending between 1.83 and 2.90 seconds (excluding the drone movement time) before initiating the drone movements. Similarly, speech commands, for instance, 'Go up slowly to an altitude of 10 meters' or 'Go North until you see a red truck below', pose long input times [48]. In contrast, our on-finger tangible interface enables continual and swift commands following the thumb press and wrist rotation. The users can finish the unit tasks (T1 – T4) within 2.91 to 3.30 seconds. Besides, users with the prototype system perform unnoticeable thumb presses on the on-finger prototype with subtle wrist rotations (pitch: 43.24° amplitude and roll: 46.35° amplitude). Our prototype enables off-handed interaction ubiquitously, for instance, under a desk indoor, as well as reserving one hand in mobile scenarios. In comparison, other existing works exploiting the body's lean angle [40], voice commands, and two-armed movements [60, 63] make obvious actions leading to social awkwardness.

6.4.2 Design Implications. The rising number of Finger-Augmenting Devices (FAD) [69] in recent years raises the open question of 'What can we do on a finger-worn interface?'. This paper serves as a groundwork for single-handed drone control within the finger space, with the following spotlights. First, rather than an opportunistic approach to putting sensors together, we systematically measure the interaction areas in Section 4 and 5 and relate them to the form factor of FADs to focus our design. Second, the design choices of IMU-induced movements between 1-level (M3) and 2-level (M4) approaches improve our understandings of multi-modal inputs for 6-DOF drone movements, especially when an additional modality (force-assisted interaction in this paper) can control the magnitude of these movements. Third, our device for thumb-based drone control inherits the benefits of subtle and unnoticeable interaction [50] from the design clues found in the first and second evaluations. In the final evaluation, the users with the hardware prototype perform gentle pitch (43.24° amplitude) and roll gestures (46.35° amplitude). Finally, our prototype is a uniquely convenient attachment on the most flexible part of the human body, enabling the users to employ the multiple modalities considered in this paper easily. Accordingly, the prototype leverages the synergy from both the natural (wrist rotation) and tangible (on-finger hardware) interfaces, leading to intuitiveness [22] and responsiveness [50]. The light-weight prototype can work with

output interfaces on the drones such as Drone.IO [19, 21], acting as an auxiliary screen for the limited screen real estate on nowadays augmented reality smartglasses [52] to display user-centric contents [47].

6.4.3 Limitations. The fundamental goal of this paper is to investigate the effects of the combination of IMU-induced and force-assisted interaction for the direct position control of a drone, beyond the most commonly used touch-based inputs. Throughout the three evaluation-phases, this paper shows evidence that the employed modalities can effectively shrink the required space of interaction such as subtle wrist rotations as well as miniature-sized dense interaction footprints. However, in search of subtle interactions on a small-sized device, the unit tasks mainly focus on pitch and roll gestures driving the horizontal and rotational drone movements. As the thoroughly studied joystick interfaces are widely applied in nowadays video gaming [72], the unit tests with a flying drone on a horizontal plane (i.e. lateral and longitudinal movements) are neglected in the paper. For future works, we will conduct experiments with the selected method M3 on the on-finger device involving multi-directional operations. For example, a most recent study using a two-handed controller serves as a discussion opener of investigating the difficulties of operating a drone to land on various target widths [80]. It would be interesting to see the user performance with our proposed methods for landing operations and further quantitatively compare the approaches under the predictive model of Fitts's Law. Additionally, we will improve the dimension of the touch-based interactions on our prototype through building flexible interfaces[9]. We will further elicit the user feedback of multi-modal inputs on textile-like surfaces, for instance, a glove.

7 CONCLUSION

Drone interaction is a new and vastly unexplored research area. Currently, most systems rely on two-handed systems, whether through a physical joystick or a smartphone app, to handle the six degrees of freedom of drone control. Although this kind of system is intuitive to the users and has been commonly used for decades in sedentary video gaming, occupying both hands does not translate well in an outdoor context. This paper serves as the first study to explore the one-handed interaction approach by exploiting force interaction and IMUs for drone control. We first evaluated several methods and compared them to the commercial baseline through both unit tests and complex tasks. We then considered the methods providing the best compromise between task completion speed, interaction area size, and user-perceived load. We selected the third method that can achieve subtle wrist movements with pitch gesture (46.89° amplitude) and roll gesture (49.19° amplitude) within a miniature-size area of (1.08 * 0.61 cm^2). We finally implemented this method within a ring-sized device. This device combines a pressure sensor with an IMU to control a drone through subtle pressure of the thumb and movements of the finger. Our results show that the ring implementation results in very similar performance and wrist postures than its implementation on smartphones. Furthermore, our Technology Acceptance Survey shows that users had a satisfying experience with the ring controller. Participants found the device easy to use ($\bar{M}$ = 3.58) and easy to learn ($\bar{M}$ = 3.58), and considered the prototype useful to control a drone ($\bar{M}$ = 3.67), especially for a mobile scenario ($\bar{M}$ = 3.92). On the premise of subtle interaction within the miniature-size interface, we plan to expand this study to wider implications, including applying the design clues to finer movements, evaluating the impact of Fitts's law on such miniature interfaces, and broadening to other smart devices such as smart wearables.

ACKNOWLEDGMENTS

This research has been supported in part by the Academy of Finland 6Genesis Flagship (grant 318927)/ 5GEAR & project 16214817 from the Research Grants Council of Hong Kong.

[9]Building interactive textile-based interfaces with Arduino and JavaScript: https://medium.com/@devdevcharlie/building-interactive-textile-based-interfaces-with-arduino-and-javascript-edf89c8d756a

REFERENCES

[1] L A Jones and S J Lederman. 2006. *Human Hand Function*. Vol. 32. https://doi.org/10.1093/acprof:oso/9780195173154.001.0001

[2] Muhammad Abdullah, Minji Kim, Waseem Hassan, Yoshihiro Kuroda, and Seokhee Jeon. 2017. HapticDrone: An Encountered-Type Kinesthetic Haptic Interface with Controllable Force Feedback: Initial Example for 1D Haptic Feedback. In *Adjunct Publication of the 30th Annual ACM Symposium on User Interface Software and Technology (UIST '17)*. ACM, New York, NY, USA, 115–117. https://doi.org/10.1145/3131785.3131821

[3] Parastoo Abtahi, Benoit Landry, Jackie (Junrui) Yang, Marco Pavone, Sean Follmer, and James A. Landay. 2019. Beyond The Force: Using Quadcopters to Appropriate Objects and the Environment for Haptics in Virtual Reality. In *Proceedings of the 2019 CHI Conference on Human Factors in Computing Systems (CHI '19)*. ACM, New York, NY, USA, Article 359, 13 pages. https://doi.org/10.1145/3290605.3300589

[4] Parastoo Abtahi, David Y. Zhao, Jane L. E., and James A. Landay. 2017. Drone Near Me: Exploring Touch-Based Human-Drone Interaction. *Proc. ACM Interact. Mob. Wearable Ubiquitous Technol.* 1, 3, Article 34 (Sept. 2017), 8 pages. https://doi.org/10.1145/3130899

[5] Charlie Anderson, Benji Barash, Charlie McNeill, Denis Ogun, Michael Wray, Jarrod Knibbe, Christopher H. Morris, and Sue Ann Seah. 2015. The Cage: Towards a 6-DoF Remote Control with Force Feedback for UAV Interaction. In *Proceedings of the 33rd Annual ACM Conference Extended Abstracts on Human Factors in Computing Systems (CHI EA '15)*. ACM, New York, NY, USA, 1687–1692. https://doi.org/10.1145/2702613.2732877

[6] Axel Antoine, Sylvain Malacria, and Géry Casiez. 2017. ForceEdge: Controlling Autoscroll on Both Desktop and Mobile Computers Using the Force. In *Proceedings of the 2017 CHI Conference on Human Factors in Computing Systems (CHI '17)*. ACM, New York, NY, USA, 3281–3292. https://doi.org/10.1145/3025453.3025605

[7] Jatin Arora, Kartik Mathur, Aryan Saini, and Aman Parnami. 2019. Gehna: Exploring the Design Space of Jewelry As an Input Modality. In *Proceedings of the 2019 CHI Conference on Human Factors in Computing Systems (CHI '19)*. ACM, New York, NY, USA, Article 521, 12 pages. https://doi.org/10.1145/3290605.3300751

[8] Mehmet Aydin Baytas, Damla undefineday, Yuchong Zhang, Mohammad Obaid, Asim Evren Yantaç, and Morten Fjeld. 2019. The Design of Social Drones: A Review of Studies on Autonomous Flyers in Inhabited Environments. In *Proceedings of the 2019 CHI Conference on Human Factors in Computing Systems (CHI '19)*. Association for Computing Machinery, New York, NY, USA, Article Paper 250, 13 pages. https://doi.org/10.1145/3290605.3300480

[9] Roger Boldu, Alexandru Dancu, Denys J.C. Matthies, Pablo Gallego Cascón, Shanaka Ransir, and Suranga Nanayakkara. 2018. Thumb-In-Motion: Evaluating Thumb-to-Ring Microgestures for Athletic Activity. In *Proceedings of the Symposium on Spatial User Interaction (SUI '18)*. ACM, New York, NY, USA, 150–157. https://doi.org/10.1145/3267782.3267796

[10] Sebastian Boring, David Ledo, Xiang 'Anthony' Chen, Nicolai Marquardt, Anthony Tang, and Saul Greenberg. 2012. The Fat Thumb: Using the Thumb's Contact Size for Single-handed Mobile Interaction. In *Proceedings of the 14th International Conference on Human-computer Interaction with Mobile Devices and Services (MobileHCI '12)*. ACM, New York, NY, USA, 39–48. https://doi.org/10.1145/2371574.2371582

[11] Sean Braley, Calvin Rubens, Timothy Merritt, and Roel Vertegaal. 2018. GridDrones: A Self-Levitating Physical Voxel Lattice for Interactive 3D Surface Deformations. In *Proceedings of the 31st Annual ACM Symposium on User Interface Software and Technology (UIST '18)*. Association for Computing Machinery, New York, NY, USA, 87–98. https://doi.org/10.1145/3242587.3242658

[12] Stephen A. Brewster and Michael Hughes. 2009. Pressure-based Text Entry for Mobile Devices. In *Proceedings of the 11th International Conference on Human-Computer Interaction with Mobile Devices and Services (MobileHCI '09)*. ACM, New York, NY, USA, Article 9, 4 pages. https://doi.org/10.1145/1613858.1613870

[13] Jessica R. Cauchard, Jane L. E, Kevin Y. Zhai, and James A. Landay. 2015. Drone and Me: An Exploration into Natural Human-drone Interaction. In *Proceedings of the 2015 ACM International Joint Conference on Pervasive and Ubiquitous Computing (UbiComp '15)*. ACM, New York, NY, USA, 361–365. https://doi.org/10.1145/2750858.2805823

[14] Jessica R. Cauchard, Alex Tamkin, Cheng Yao Wang, Luke Vink, Michelle Park, Tommy Fang, and James A. Landay. 2019. Drone.IO: A Gestural and Visual Interface for Human-Drone Interaction. In *Proceedings of the 14th ACM/IEEE International Conference on Human-Robot Interaction (HRI '19)*. IEEE Press, 153–162.

[15] Jessica Rebecca Cauchard, Kevin Y. Zhai, Marco Spadafora, and James A. Landay. 2016. Emotion Encoding in Human-Drone Interaction. In *The Eleventh ACM/IEEE International Conference on Human Robot Interaction (HRI '16)*. IEEE Press, 263–270.

[16] Edwin Chan, Teddy Seyed, Wolfgang Stuerzlinger, Xing-Dong Yang, and Frank Maurer. 2016. User Elicitation on Single-hand Microgestures. In *Proceedings of the 2016 CHI Conference on Human Factors in Computing Systems (CHI '16)*. ACM, New York, NY, USA, 3403–3414. https://doi.org/10.1145/2858036.2858589

[17] Liwei Chan, Rong-Hao Liang, Ming-Chang Tsai, Kai-Yin Cheng, Chao-Huai Su, Mike Y. Chen, Wen-Huang Cheng, and Bing-Yu Chen. 2013. FingerPad: Private and Subtle Interaction Using Fingertips. In *Proceedings of the 26th Annual ACM Symposium on User Interface Software and Technology (UIST '13)*. ACM, New York, NY, USA, 255–260. https://doi.org/10.1145/2501988.2502016

[18] Chien-Fang Chen, Kang-Ping Liu, and Neng-Hao Yu. 2015. Exploring Interaction Modalities for a Selfie Drone. In *SIGGRAPH Asia 2015 Posters (SA '15)*. ACM, New York, NY, USA, Article 25, 2 pages. https://doi.org/10.1145/2820926.2820965

[19] Yu-An Chen, Te-Yen Wu, Tim Chang, Jun You Liu, Yuan-Chang Hsieh, Leon Yulun Hsu, Ming-Wei Hsu, Paul Taele, Neng-Hao Yu, and Mike Y. Chen. 2018. ARPilot: Designing and Investigating AR Shooting Interfaces on Mobile Devices for Drone Videography. In *Proceedings of the 20th International Conference on Human-Computer Interaction with Mobile Devices and Services (MobileHCI '18)*. Association for Computing Machinery, New York, NY, USA, Article Article 42, 8 pages. https://doi.org/10.1145/3229434.3229475

[20] Christian Corsten, Marcel Lahaye, Jan Borchers, and Simon Voelker. 2019. ForceRay: Extending Thumb Reach via Force Input Stabilizes Device Grip for Mobile Touch Input. In *Proceedings of the 2019 CHI Conference on Human Factors in Computing Systems (CHI '19)*. ACM, New York, NY, USA, Article 212, 12 pages. https://doi.org/10.1145/3290605.3300442

[21] Rajkumar Darbar, Joan Sol Roo, Thibault Lainé, and Martin Hachet. 2019. DroneSAR: Extending Physical Spaces in Spatial Augmented Reality Using Projection on a Drone. In *Proceedings of the 18th International Conference on Mobile and Ubiquitous Multimedia (MUM '19)*. Association for Computing Machinery, New York, NY, USA, Article Article 4, 7 pages. https://doi.org/10.1145/3365610.3365631

[22] Maria De Marsico and Alessandro Spagnoli. 2019. Using Hands As an Easy UAV Joystick for Entertainment Applications. In *Proceedings of the 13th Biannual Conference of the Italian SIGCHI Chapter: Designing the Next Interaction (CHItaly '19)*. ACM, New York, NY, USA, Article 9, 9 pages. https://doi.org/10.1145/3351995.3352042

[23] Tinglin Duan, Parinya Punpongsanon, Daisuke Iwai, and Kosuke Sato. 2018. FlyingHand: Extending the Range of Haptic Feedback on Virtual Hand Using Drone-based Object Recognition. In *SIGGRAPH Asia 2018 Technical Briefs (SA '18)*. ACM, New York, NY, USA, Article 28, 4 pages. https://doi.org/10.1145/3283254.3283258

[24] Jane L. E, Ilene L. E, James A. Landay, and Jessica R. Cauchard. 2017. Drone Wo: Cultural Influences on Human-Drone Interaction Techniques. In *Proceedings of the 2017 CHI Conference on Human Factors in Computing Systems (CHI '17)*. Association for Computing Machinery, New York, NY, USA, 6794–6799. https://doi.org/10.1145/3025453.3025755

[25] Alexander Eiselmayer, Chat Wacharamanotham, Michel Beaudouin-Lafon, and Wendy E. Mackay. 2019. Touchstone2: An Interactive Environment for Exploring Trade-Offs in HCI Experiment Design. In *Proceedings of the 2019 CHI Conference on Human Factors in Computing Systems (CHI '19)*. Association for Computing Machinery, New York, NY, USA, Article Paper 217, 11 pages. https://doi.org/10.1145/3290605.3300447

[26] Markus Funk. 2018. Human-drone Interaction: Let's Get Ready for Flying User Interfaces! *Interactions* 25, 3 (April 2018), 78–81. https://doi.org/10.1145/3194317

[27] Sarthak Ghosh, Hyeong Cheol Kim, Yang Cao, Arne Wessels, Simon T. Perrault, and Shengdong Zhao. 2016. Ringteraction: Coordinated Thumb-index Interaction Using a Ring. In *Proceedings of the 2016 CHI Conference Extended Abstracts on Human Factors in Computing Systems (CHI EA '16)*. ACM, New York, NY, USA, 2640–2647. https://doi.org/10.1145/2851581.2892371

[28] Alix Goguey, Sylvain Malacria, and Carl Gutwin. 2018. Improving Discoverability and Expert Performance in Force-Sensitive Text Selection for Touch Devices with Mode Gauges. In *Proceedings of the 2018 CHI Conference on Human Factors in Computing Systems (CHI '18)*. ACM, New York, NY, USA, Article 477, 12 pages. https://doi.org/10.1145/3173574.3174051

[29] Boris Gromov, Luca M. Gambardella, and Alessandro Giusti. 2018. Video: Landing a Drone with Pointing Gestures. In *Companion of the 2018 ACM/IEEE International Conference on Human-Robot Interaction (HRI '18)*. ACM, New York, NY, USA, 374–374. https://doi.org/10.1145/3173386.3177530

[30] Teng Han, Qian Han, Michelle Annett, Fraser Anderson, Da-Yuan Huang, and Xing-Dong Yang. 2017. Frictio: Passive Kinesthetic Force Feedback for Smart Ring Output. In *Proceedings of the 30th Annual ACM Symposium on User Interface Software and Technology (UIST '17)*. ACM, New York, NY, USA, 131–142. https://doi.org/10.1145/3126594.3126622

[31] John Paulin Hansen, Alexandre Alapetite, I. Scott MacKenzie, and Emilie Møllenbach. 2014. The Use of Gaze to Control Drones. In *Proceedings of the Symposium on Eye Tracking Research and Applications (ETRA '14)*. ACM, New York, NY, USA, 27–34. https://doi.org/10.1145/2578153.2578156

[32] Matthias Hoppe, Marinus Burger, Albrecht Schmidt, and Thomas Kosch. 2019. DronOS: A Flexible Open-Source Prototyping Framework for Interactive Drone Routines. In *Proceedings of the 18th International Conference on Mobile and Ubiquitous Multimedia (MUM '19)*. Association for Computing Machinery, New York, NY, USA, Article Article 15, 7 pages. https://doi.org/10.1145/3365610.3365642

[33] Eva Hornecker. 2012. Beyond Affordance: Tangibles' Hybrid Nature. In *Proceedings of the Sixth International Conference on Tangible, Embedded and Embodied Interaction (TEI '12)*. Association for Computing Machinery, New York, NY, USA, 175–182. https://doi.org/10.1145/2148131.2148168

[34] Yi-Ta Hsieh, Antti Jylhä, Valeria Orso, Luciano Gamberini, and Giulio Jacucci. 2016. Designing a Willing-to-Use-in-Public Hand Gestural Interaction Technique for Smart Glasses. In *Proceedings of the 2016 CHI Conference on Human Factors in Computing Systems (CHI '16)*. Association for Computing Machinery, New York, NY, USA, 4203–4215. https://doi.org/10.1145/2858036.2858436

[35] Min-Chieh Hsiu, Da-Yuan Huang, Chi An Chen, Yu-Chih Lin, Yi-ping Hung, De-Nian Yang, and Mike Chen. 2016. ForceBoard: Using Force As Input Technique on Size-limited Soft Keyboard. In *Proceedings of the 18th International Conference on Human-Computer Interaction with Mobile Devices and Services Adjunct (MobileHCI '16)*. ACM, New York, NY, USA, 599–604. https://doi.org/10.1145/2957265.2961827

[36] NASA AMES Research Center Human Performance Research Group. 1999. NASA Task Load Index (TLX). https://humansystems.arc.nasa.gov/groups/TLX/downloads/TLX.pdf

[37] Robert J.K. Jacob, Audrey Girouard, Leanne M. Hirshfield, Michael S. Horn, Orit Shaer, Erin Treacy Solovey, and Jamie Zigelbaum. 2008. Reality-Based Interaction: A Framework for Post-WIMP Interfaces. In *Proceedings of the SIGCHI Conference on Human Factors in Computing Systems (CHI '08)*. Association for Computing Machinery, New York, NY, USA, 201–210. https://doi.org/10.1145/1357054.1357089

[38] Lei Jing, Zixue Cheng, Yinghui Zhou, Junbo Wang, and Tongjun Huang. 2013. Magic Ring: A Self-contained Gesture Input Device on Finger. In *Proceedings of the 12th International Conference on Mobile and Ubiquitous Multimedia (MUM '13)*. ACM, New York, NY, USA, Article 39, 4 pages. https://doi.org/10.1145/2541831.2541875

[39] Amy K. Karlson, Benjamin B. Bederson, and José Luis Contreras-Vidal. 2006. Studies in One-Handed Mobile Design : Habit , Desire and Agility.

[40] Md. Nafiz Hasan Khan, Carman Neustaedter, and Alissa . Antle. 2019. Flight Chair: An Interactive Chair for Controlling Emergency Service Drones. In *Extended Abstracts of the 2019 CHI Conference on Human Factors in Computing Systems (CHI EA '19)*. ACM, New York, NY, USA, Article LBW1320, 5 pages. https://doi.org/10.1145/3290607.3313031

[41] Bomyeong Kim, Hyun Young Kim, and Jinwoo Kim. 2016. Getting Home Safely with Drone. In *Proceedings of the 2016 ACM International Joint Conference on Pervasive and Ubiquitous Computing: Adjunct (UbiComp '16)*. Association for Computing Machinery, New York, NY, USA, 117–120. https://doi.org/10.1145/2968219.2971426

[42] Heesoon Kim and James A. Landay. 2018. Aeroquake: Drone Augmented Dance. In *Proceedings of the 2018 Designing Interactive Systems Conference (DIS '18)*. ACM, New York, NY, USA, 691–701. https://doi.org/10.1145/3196709.3196798

[43] Hyun Young Kim, Bomyeong Kim, and Jinwoo Kim. 2016. The Naughty Drone: A Qualitative Research on Drone As Companion Device. In *Proceedings of the 10th International Conference on Ubiquitous Information Management and Communication (IMCOM '16)*. ACM, New York, NY, USA, Article 91, 6 pages. https://doi.org/10.1145/2857546.2857639

[44] Thomas Kosch, Markus Funk, Daniel Vietz, Marc Weise, Tamara Müller, and Albrecht Schmidt. 2018. DroneCTRL: A Tangible Remote Input Control for Quadcopters. In *The 31st Annual ACM Symposium on User Interface Software and Technology Adjunct Proceedings (UIST '18 Adjunct)*. ACM, New York, NY, USA, 120–122. https://doi.org/10.1145/3266037.3266121

[45] Nataliya Kos'myna, Franck Tarpin-Bernard, and Bertrand Rivet. 2014. Bidirectional Feedback in Motor Imagery BCIs: Learn to Control a Drone Within 5 Minutes. In *CHI '14 Extended Abstracts on Human Factors in Computing Systems (CHI EA '14)*. ACM, New York, NY, USA, 479–482. https://doi.org/10.1145/2559206.2574820

[46] Joseph La Delfa, Mehmet Aydin Baytas, Olivia Wichtowski, Rohit Ashok Khot, and Florian Floyd Mueller. 2019. Are Drones Meditative?. In *Extended Abstracts of the 2019 CHI Conference on Human Factors in Computing Systems (CHI EA '19)*. Association for Computing Machinery, New York, NY, USA, Article Paper INT046, 4 pages. https://doi.org/10.1145/3290607.3313274

[47] Kit-Yung Lam, Lik-Hang Lee, Tristan Braud, and Pan Hui. 2019. M2A: A Framework for Visualizing Information from Mobile Web to Mobile Augmented Reality. In *2019 IEEE International Conference on Pervasive Computing and Communications (PerCom*. 1–10. https://doi.org/10.1109/PERCOM.2019.8767388

[48] Megan Landau and Sebastian van Delden. 2017. A System Architecture for Hands-Free UAV Drone Control Using Intuitive Voice Commands. In *Proceedings of the Companion of the 2017 ACM/IEEE International Conference on Human-Robot Interaction (HRI '17)*. ACM, New York, NY, USA, 181–182. https://doi.org/10.1145/3029798.3038329

[49] Huy Viet Le, Sven Mayer, Patrick Bader, and Niels Henze. 2018. Fingers' Range and Comfortable Area for One-Handed Smartphone Interaction Beyond the Touchscreen. In *Proceedings of the 2018 CHI Conference on Human Factors in Computing Systems (CHI '18)*. ACM, New York, NY, USA, Article 31, 12 pages. https://doi.org/10.1145/3173574.3173605

[50] Lik-Hang Lee and Pan Hui. 2018. Interaction Methods for Smart Glasses: A Survey. *IEEE Access* 6 (2018), 28712–28732. https://doi.org/10.1109/ACCESS.2018.2831081

[51] Lik-Hang Lee, Kit-Yung Lam, Tong Li, Tristan Braud, Xiang Su, and Pan Hui. 2019. Quadmetric Optimized Thumb-to-Finger Interaction for Force Assisted One-Handed Text Entry on Mobile Headsets. *Proc. ACM Interact. Mob. Wearable Ubiquitous Technol.* 2, 4, Article 201 (Dec. 2019), 21 pages. https://doi.org/10.1145/3287079

[52] Lik-Hang Lee, Kit-Yung Lam, Yui-Pan Yau, Tristan Braud, and Pan Hui. 2019. HIBEY: Hide the Keyboard in Augmented Reality. In *2019 IEEE International Conference on Pervasive Computing and Communications (PerCom*. 1–10.

[53] Lik-Hang Lee, Yiming Zhu, Yui-Pan Yau, Tristan Braud, Xiang Su, and Pan Hui. 2020. One-thumb Text Acquisition on Force-assisted Miniature Interfaces for Mobile Headsets. In *2020 IEEE International Conference on Pervasive Computing and Communications (PerCom*. 1–10.

[54] Hannah Limerick, James W. Moore, and David Coyle. 2015. Empirical Evidence for a Diminished Sense of Agency in Speech Interfaces. In *Proceedings of the 33rd Annual ACM Conference on Human Factors in Computing Systems (CHI '15)*. Association for Computing Machinery, New York, NY, USA, 3967–3970. https://doi.org/10.1145/2702123.2702379

[55] J. M. M. L., Jolley. 2010. *Research design explained: Instructor's edition (7th ed.)*. Wadsworth/Cengage Learning.

[56] I. Scott MacKenzie. 2013. *Human-Computer Interaction: An Empirical Research Perspective* (1st ed.). Morgan Kaufmann Publishers Inc., San Francisco, CA, USA.

[57] Wenguang Mao, Zaiwei Zhang, Lili Qiu, Jian He, Yuchen Cui, and Sangki Yun. 2017. Indoor Follow Me Drone. In *Proceedings of the 15th Annual International Conference on Mobile Systems, Applications, and Services (MobiSys '17)*. Association for Computing Machinery, New

York, NY, USA, 345–358. https://doi.org/10.1145/3081333.3081362
[58] Silvia Mirri, Catia Prandi, and Paola Salomoni. 2019. Human-Drone Interaction: State of the Art, Open Issues and Challenges. In *Proceedings of the ACM SIGCOMM 2019 Workshop on Mobile AirGround Edge Computing, Systems, Networks, and Applications (MAGESys'19)*. ACM, New York, NY, USA, 43–48. https://doi.org/10.1145/3341568.3342111
[59] Sachi Mizobuchi, Shinya Terasaki, Turo Keski-Jaskari, Jari Nousiainen, Matti Ryynanen, and Miika Silfverberg. 2005. Making an Impression: Force-controlled Pen Input for Handheld Devices. In *CHI '05 Extended Abstracts on Human Factors in Computing Systems (CHI EA '05)*. ACM, New York, NY, USA, 1661–1664. https://doi.org/10.1145/1056808.1056991
[60] Koji Morishita, Hiroaki Yanagisawa, and Hisashi Noda. 2016. Intuitive Control for Moving Drones. In *SIGGRAPH ASIA 2016 Posters (SA '16)*. ACM, New York, NY, USA, Article 17, 2 pages. https://doi.org/10.1145/3005274.3005287
[61] Donald A. Norman. 2010. Natural User Interfaces Are Not Natural. *Interactions* 17, 3 (May 2010), 6–10. https://doi.org/10.1145/1744161.1744163
[62] Sarah North, Adnan Rashied, Jason Walters, Ahmad Alissa, Josh Cooper, Eric Rawls, Cheyenne Sancho, Utku "Victor" Sahin, Kate Randell, and Heather Rego. 2018. Performance Analysis of Brain-computer Interfaces in Aerial Drone. In *Proceedings of the ACMSE 2018 Conference (ACMSE '18)*. ACM, New York, NY, USA, Article 16, 5 pages. https://doi.org/10.1145/3190645.3190683
[63] Mohammad Obaid, Felix Kistler, Gabrielė Kasparavičiūtė, Asim Evren Yantaç, and Morten Fjeld. 2016. How Would You Gesture Navigate a Drone?: A User-centered Approach to Control a Drone. In *Proceedings of the 20th International Academic Mindtrek Conference (AcademicMindtrek '16)*. ACM, New York, NY, USA, 113–121. https://doi.org/10.1145/2994310.2994348
[64] Judith S. Olson and Wendy A. Kellogg. 2014. *Ways of Knowing in HCI*. Springer Publishing Company, Incorporated.
[65] Anne Roudaut, Stéphane Huot, and Eric Lecolinet. 2008. TapTap and MagStick: Improving One-handed Target Acquisition on Small Touch-screens. In *Proceedings of the Working Conference on Advanced Visual Interfaces (AVI '08)*. ACM, New York, NY, USA, 146–153. https://doi.org/10.1145/1385569.1385594
[66] Carlos Ruiz, Shijia Pan, Adeola Bannis, Xinlei Chen, Carlee Joe-Wong, Hae Young Noh, and Pei Zhang. 2018. IDrone: Robust Drone Identification through Motion Actuation Feedback. *Proc. ACM Interact. Mob. Wearable Ubiquitous Technol.* 2, 2, Article Article 80 (July 2018), 22 pages. https://doi.org/10.1145/3214283
[67] Lucian Alexandru Sandru, Marius Florin Crainic, Diana Savu, Cristian Moldovan, Valer Dolga, and Stefan Preitl. 2016. Automatic Control of a Quadcopter, AR. Drone, Using a Smart Glove. In *Proceedings of the 4th International Conference on Control, Mechatronics and Automation (ICCMA '16)*. ACM, New York, NY, USA, 92–98. https://doi.org/10.1145/3029610.3029619
[68] Matthias Seuter, Eduardo Rodriguez Macrillante, Gernot Bauer, and Christian Kray. 2018. Running with Drones: Desired Services and Control Gestures. In *Proceedings of the 30th Australian Conference on Computer-Human Interaction (OzCHI '18)*. ACM, New York, NY, USA, 384–395. https://doi.org/10.1145/3292147.3292156
[69] Roy Shilkrot, Jochen Huber, Jürgen Steimle, Suranga Nanayakkara, and Pattie Maes. 2015. Digital Digits: A Comprehensive Survey of Finger Augmentation Devices. *ACM Comput. Surv.* 48, 2, Article 30 (Nov. 2015), 29 pages. https://doi.org/10.1145/2828993
[70] Mohamed Soliman, Franziska Mueller, Lena Hegemann, Joan Sol Roo, Christian Theobalt, and Jürgen Steimle. 2018. FingerInput: Capturing Expressive Single-Hand Thumb-to-Finger Microgestures. In *Proceedings of the 2018 ACM International Conference on Interactive Surfaces and Spaces (ISS '18)*. ACM, New York, NY, USA, 177–187. https://doi.org/10.1145/3279778.3279799
[71] Hong Tan, J. Radcliffe, Book No. Ga, Hong Z. Tan, Brian Eberman, Mandayam A. Srinivasan, and Belinda Cheng. 1994. Human Factors For The Design Of Force-Reflecting Haptic Interfaces.
[72] Robert J. Teather, Andrew Roth, and I. Scott MacKenzie. 2017. Tilt-Touch synergy: Input control for "dual-analog" style mobile games. *Entertainment Computing* 21 (2017), 33 – 43. https://doi.org/10.1016/j.entcom.2017.04.005
[73] Ryotaro Temma, Kazuki Takashima, Kazuyuki Fujita, Koh Sueda, and Yoshifumi Kitamura. 2019. Third-Person Piloting: Increasing Situational Awareness Using a Spatially Coupled Second Drone. In *Proceedings of the 32nd Annual ACM Symposium on User Interface Software and Technology (UIST '19)*. Association for Computing Machinery, New York, NY, USA, 507–519. https://doi.org/10.1145/3332165.3347953
[74] D. Tezza and M. Andujar. 2019. The State-of-the-Art of Human–Drone Interaction: A Survey. *IEEE Access* 7 (2019), 167438–167454. https://doi.org/10.1109/ACCESS.2019.2953900
[75] Asher Trockman. 2015. 3D Touch: Sensitivity, Force vs. Weight.
[76] Hsin-Ruey Tsai, Min-Chieh Hsiu, Jui-Chun Hsiao, Lee-Ting Huang, Mike Chen, and Yi-Ping Hung. 2016. TouchRing: Subtle and Always-available Input Using a Multi-touch Ring. In *Proceedings of the 18th International Conference on Human-Computer Interaction with Mobile Devices and Services Adjunct (MobileHCI '16)*. ACM, New York, NY, USA, 891–898. https://doi.org/10.1145/2957265.2961860
[77] Cheng-Yao Wang, Wei-Chen Chu, Po-Tsung Chiu, Min-Chieh Hsiu, Yih-Harn Chiang, and Mike Y. Chen. 2015. PalmType: Using Palms As Keyboards for Smart Glasses. In *Proceedings of the 17th International Conference on Human-Computer Interaction with Mobile Devices and Services (MobileHCI '15)*. ACM, New York, NY, USA, 153–160. https://doi.org/10.1145/2785830.2785886
[78] Eric Whitmire, Mohit Jain, Divye Jain, Greg Nelson, Ravi Karkar, Shwetak Patel, and Mayank Goel. 2017. DigiTouch: Reconfigurable Thumb-to-Finger Input and Text Entry on Head-mounted Displays. *Proc. ACM Interact. Mob. Wearable Ubiquitous Technol.* 1, 3, Article 113 (Sept. 2017), 21 pages. https://doi.org/10.1145/3130978

[79] Anna Wojciechowska, Jeremy Frey, Esther Mandelblum, Yair Amichai-Hamburger, and Jessica R. Cauchard. 2019. Designing Drones: Factors and Characteristics Influencing the Perception of Flying Robots. *Proc. ACM Interact. Mob. Wearable Ubiquitous Technol.* 3, 3, Article Article 111 (Sept. 2019), 19 pages. https://doi.org/10.1145/3351269

[80] Kaito Yamada, Hiroki Usuba, and Homei Miyahita. 2019. Modeling Drone Pointing Movement with Fitts' Law. In *Extended Abstracts of the 2019 CHI Conference on Human Factors in Computing Systems (CHI EA '19)*. ACM, New York, NY, USA, Article LBW2519, 6 pages. https://doi.org/10.1145/3290607.3312835

[81] Yaxing Yao, Huichuan Xia, Yun Huang, and Yang Wang. 2017. Privacy Mechanisms for Drones: Perceptions of Drone Controllers and Bystanders. In *Proceedings of the 2017 CHI Conference on Human Factors in Computing Systems (CHI '17)*. Association for Computing Machinery, New York, NY, USA, 6777–6788. https://doi.org/10.1145/3025453.3025907

[82] Jibin Yin, Xiangshi Ren, and Shumin Zhai. 2010. Pen Pressure Control in Trajectory-based Interaction. *Behav. Inf. Technol.* 29, 2 (March 2010), 137–148. https://doi.org/10.1080/01449290902904733

[83] Mingyuan Zhong, Chun Yu, Qian Wang, Xuhai Xu, and Yuanchun Shi. 2018. ForceBoard: Subtle Text Entry Leveraging Pressure. In *Proceedings of the 2018 CHI Conference on Human Factors in Computing Systems (CHI '18)*. ACM, New York, NY, USA, Article 528, 10 pages. https://doi.org/10.1145/3173574.3174102